



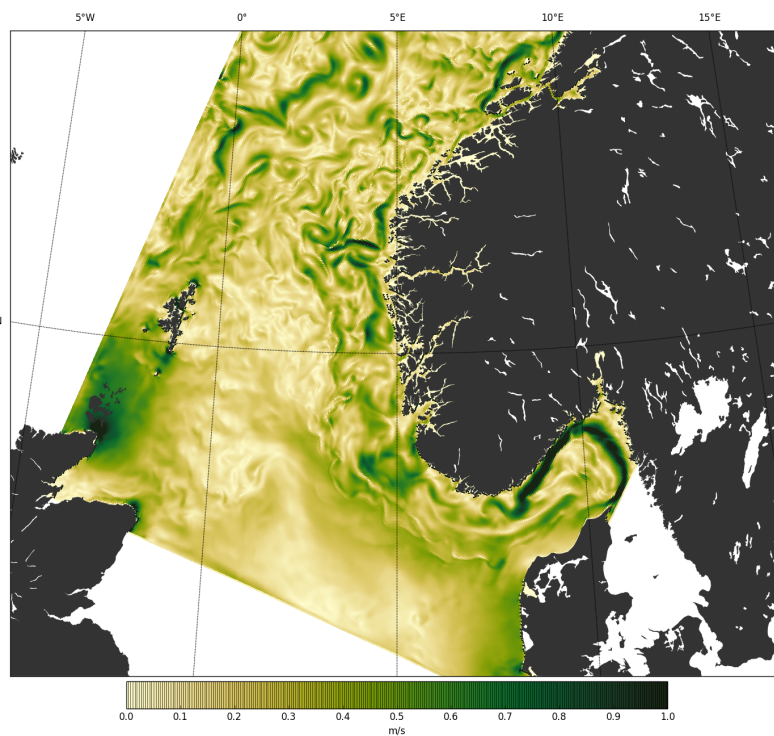
Norwegian
Meteorological
Institute

METreport

No. 04/2018
ISSN 2387-4201
Oceanography

NorShelf: A reanalysis and data-assimilative forecast model for the Norwegian Shelf Sea

Documentation of ocean model setup
Johannes Röhrs, Ann Kristin Sperrevik and Kai H. Christensen





Norwegian
Meteorological
Institute

METreport

Title NorShelf: An ocean reanalysis and data-assimilative forecast model for the Norwegian Shelf Sea	Date December 14, 2018
Section Oceanography	Report no. 04/2018
Author(s) Johannes Röhrs, Ann Kristin Sperrevik, Kai H. Christensen	Classification <input checked="" type="radio"/> Free <input type="radio"/> Restricted
Client(s)	Client's reference
Abstract A regional ocean model setup with data assimilation (DA) for the shelf sea off Norway has been set up at the Norwegian Meteorological Institute (MET Norway). The model domain includes the Skagerrak in the southeast, the northern parts of the North Sea, the Shelf sea off western Norway including the shelf slope, and parts of the Barents Sea in the north. NorShelf is based on the Regional Ocean Modeling System (ROMS) with a physical space 4D-variational (4D-Var) DA scheme. A horizontal model resolution of 2.4km has been chosen to suit the scale of the available observations, and to compromise the need to resolve high resolution eddy dynamics while confining nonlinearities that limit the 4D-Var DA capabilities. The model is intended as forecasting tool for ocean circulation and hydrography beyond the coastal area, including the entire shelf sea and the dynamics of the North Atlantic current at the shelf slope. This report contains a full description of model configuration and examples of model hydrography and 4D-Var performance.	
Keywords Ocean model, ROMS, 4D-Var data assimilation	

Disciplinary signature
Øyvind Breivik

Responsible signature
Kai H. Christensen

Contents

1	Motivation	4
2	Setup of the ocean model ROMS	5
2.1	Domain and model bathymetry	5
2.2	Vertical grid	5
2.3	Boundary conditions	8
2.4	Surface forcing	9
2.5	River forcing	9
2.6	Tidal forcing	10
2.7	Subscale processes	10
2.8	Time stepping and advection schemes	11
3	The NorShelf reanalysis	12
3.1	Observations	12
3.2	The 4D-Var setup	12
4	The operational forecast suite	13
4.1	Observations	14
4.2	The 4D-Var setup	14
5	Examples	14
5.1	Reanalysis	14
5.2	Analysis and forecast	26
6	Dissemination of reanalysis and forecast data	33
7	Discussion and Outlook	36
8	Acknowledgements	37

1 Motivation

The analysis and forecasting of ocean currents and hydrography is part of the Norwegian Meteorological Institutes (MET Norway) national responsibilities to secure life and values. The main applications of ocean modeling in the context of forecasting are Search-and-Rescue at sea (*Breivik et al.*, 2013), oil spill modelling (e.g. *Röhrs et al.*, 2018) and plankton transport (e.g. *Strand et al.*, 2017). For these purposes, ocean surface currents are the most central forecast parameter. *Sperrevik et al.* (2017) show that an accurate description of ocean hydrography and stratification is required for realistic modeling of ocean surface currents and trajectories. Hence, prediction of temperature and salinity throughout the water column become relevant for short term prediction. Sea surface temperature (SST) from ocean forecast models are furthermore useful as forcing for numerical weather prediction models.

Data assimilation (DA) has long been recognized as central for providing predictive skill in weather prediction. In operational ocean modeling, use of DA has been hampered by lack of real-time observations and the smaller scale of meso-scale circulation features compared to atmospheric applications. For the North Atlantic, several DA ocean model systems for basin-wide scales, with horizontal model resolution around 10km, have existed for the last 10 years, e.g. the TOPAZ model for the North Atlantic and Arctic ocean (*Xie et al.*, 2017) and the FOAM Atlantic Margin Model for the European Northwest Shelf (*Wakelin et al.*, 2009). In this work, a regional, meso-scale, eddy-permitting ocean model at 2.4km resolution for the coastal and shelf sea off Norway is presented.

The NorShelf model is particularly intended for the short-term prediction of surface currents and hydrography on the continental shelf. Operational observations of these variables in the Norwegian Sea are sparse. Surface currents are observed from a limited number of HF radars along the coast of Norway, at present there are 3 stations. Sea surface temperature (SST) measured by satellites is available on a daily basis, covering all cloud free regions. Hydrography is provided by CTD sections from occasional research cruises, ferry boxes, and ARGO floats, in addition to few experimental glider and wave buoy surveys. The role of the ocean model with DA is to fill the gaps in observation networks, hence providing knowledge of actual hydrography beyond the parts covered by observations.

For horizontal resolution in NorShelf, 2.4 km is chosen as a compromise between the need for linearization in 4D-var DA and level of detail in the forecasts. This is considered to be an intermediate scale, compared to higher resolution coastal models and lower resolution basin scale models. The order of 1km is also considered to be suitable for DA because most oceanic observations do not provide information on smaller scales.

The model region, the entire Shelf Sea off Norway in addition to the Skagerrak, the northern North Sea and the southern Barents Sea is chosen. Within the responsibility of MET Norway, the most pertinent incidents that require oceanic forecasts occur in this region close to the coast and on the continental shelf. This is also the region that most of the available in-situ observations in Norway cover. For the Arctic, a separate forecast system is being developed.

The main downstream use of the oceanic forecast from the NorShelf model system will

be to provide input for trajectory models (*Dagestad et al., 2018*) and boundary conditions for higher resolution models that focus on the near-shore and fjords.

This report contains a description of all model configurations that are needed to setup ROMS. Examples of temperature and salinity distributions are shown in terms of surface fields and vertical sections. Differences between model runs with and without 4D-Var DA are briefly discussed. Finally, a few diagnostics that evaluate the performance of the 4D-Var system are presented. The report aims to provide a detailed description of how the model is setup and configured and to display some overall results in a nutshell. An in-depth model evaluation and scientific discussion of the 4D-Var system are beyond the scope of this report.

2 Setup of the ocean model ROMS

NorShelf is built on the Regional Ocean Modeling System (ROMS), which is characterized by using a topography following coordinate system in the vertical (*Shchepetkin and McWilliams, 2005*) and extended capabilities for 4D-var DA (*Moore et al., 2011*). ROMS solves the Boussinesq primitive equations. The modeled state variables are temperature, salinity, surface elevation, and horizontal current velocities. The setup in NorShelf includes a second order turbulence closure scheme with turbulent kinetic energy and a generic length scale as state variables (*Warner et al., 2005*).

All model configurations that are set during compiling are listed in the Appendix A, and exemplary model configurations that are set at run-time are listed in the Appendix B.

2.1 Domain and model bathymetry

The model domain is shown in Fig. 1. The model resolution is approximately 2.4km, which varies slightly throughout the domain consisting of 900 x 350 grid points. The bathymetry is based on the GEBCO global data set and interpolated to the model grid. Minimum depth is set to 10m. The bathymetry is smoothed to reduce pressure gradient errors as required in ROMS. Near the boundaries, the bathymetry and coastlines are modified to avoid numerical instabilities near complex features. Additionally, the coastline has been modified to match numerical grid point criteria by ROMS (i.e. every water grid point must have at least two adjacent open boundaries). The raw and filtered bathymetries are shown in Fig. 2, however they only differ on local scales in places where bathymetry is very steep or irregular.

2.2 Vertical grid

ROMS is based on stretched, topography-following vertical coordinates. NorShelf uses 42 vertical layers with emphasis on the upper mixed layer using the ROMS-specific parameters as shown in Tab. 1. This choice of parameters results in an upper layer of approx. 0.2-1.2m and maintains an increased resolution in the upper 100m. Vertical coordinate lines at the Torungen-Hirtshals section are shown in Fig. 3 for the upper 100m.

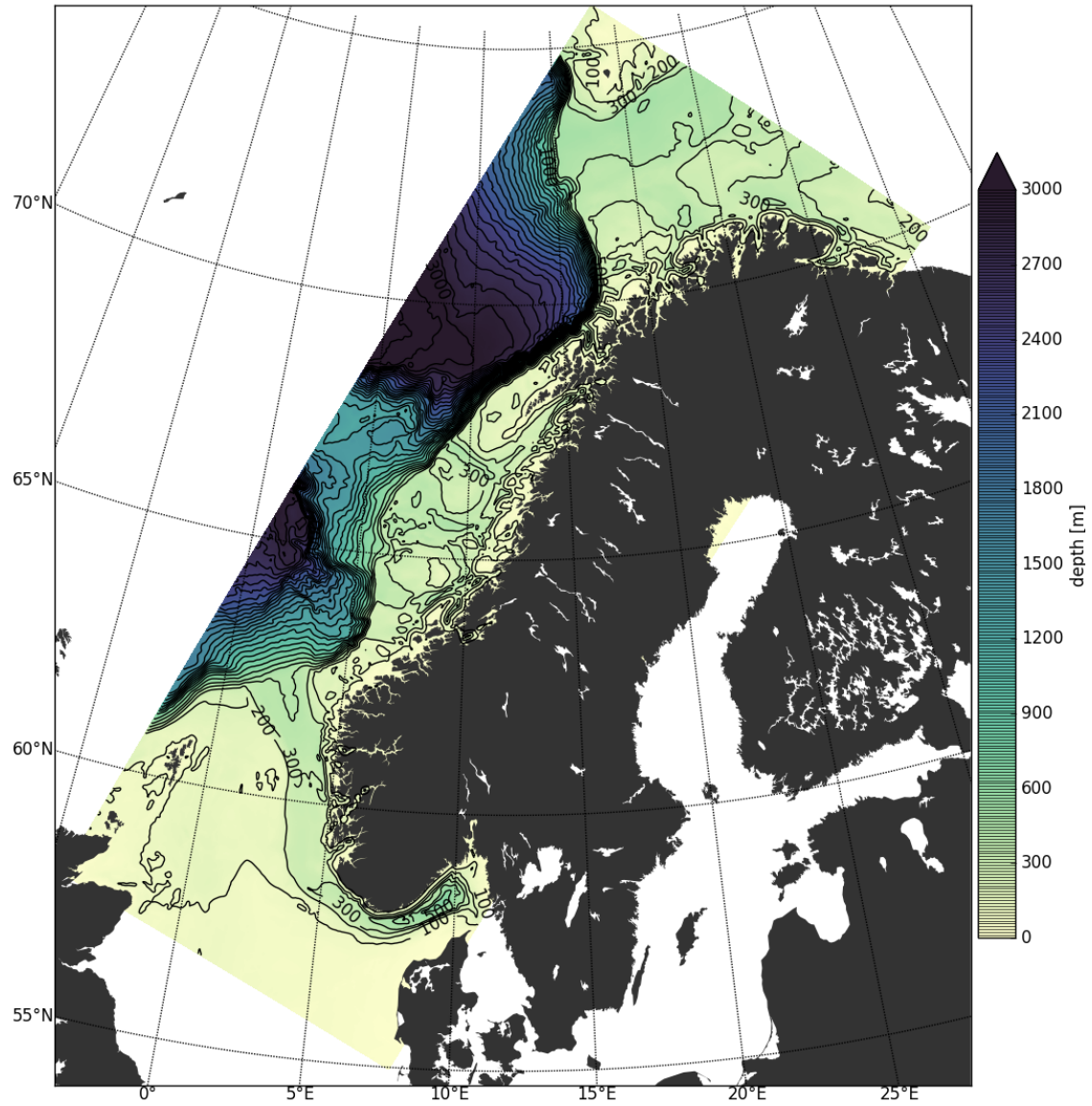


Figure 1: Domain and bathymetry of the NorShelf model model

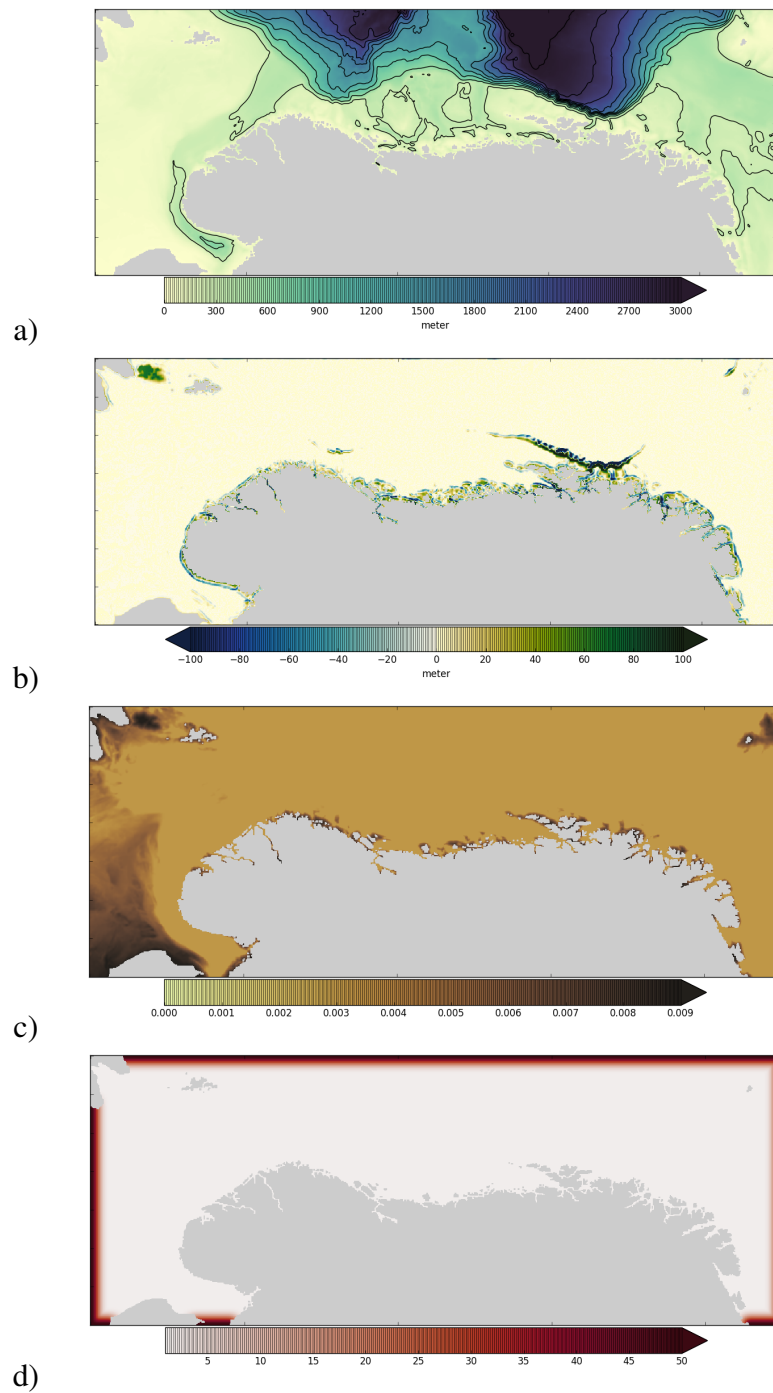


Figure 2: a) Smoothed model bathymetry of the NorShelf model. b) Difference between smoothed and raw bathymetry. c) Quadratic bottom drag coefficient. d) Diffusivity factor used for horizontal diffusion of tracers.

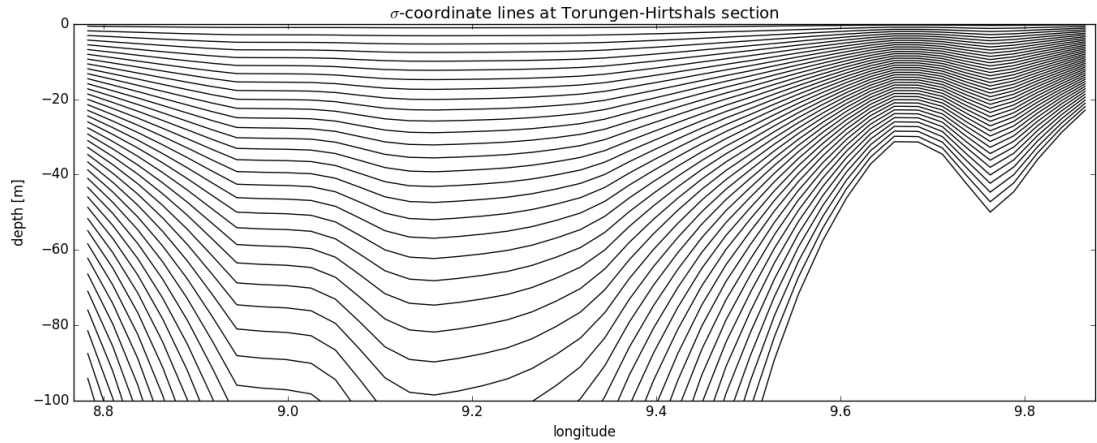


Figure 3: Lines of constant vertical coordinate for the Torungen-Hirtshals section (Fig. 7. At this section, the uppermost layer varies between a thickness of 0.2m in the shallowest part and 1m at a depth of 500m.)

Transform function	Stretching function	θ_S	θ_B	H_c
2	4	6.	0.3	100m

Table 1: Parameters for the setup of the topography following vertical coordinate

2.3 Boundary conditions

The boundary conditions for NorShelf are provided by TOPAZ version 4, a coupled ocean and sea ice DA system based on the HYCOM ocean model and the ensemble Kalman filter DA method. It is configured for the North Atlantic and Arctic Ocean with a horizontal resolution of 12-16km (Xie *et al.*, 2017), and provides daily averages of temperature, salinity, surface elevation and ocean current velocities. Since TOPAZ does not include forcing by atmospheric pressure, the inverse barometric effect due to the local atmospheric pressure is added to the sea surface elevation boundary conditions.

The numerical boundary layer schemes used to impose the various state variables at the boundary are given in Tab. 2. Note that the 4D-var analysis use different boundary conditions schemes.

Variable	hindcast/forecast	4D-var analysis/reanalysis
free surface	Chapman explicit	Chapman implicit
2D momentum	Shchepetkin	Flather
3D momentum	oblique radiation and nudging	clamped
salinity and temperature	oblique radiation with nudging	clamped
TKE and GLS	gradient	gradient

Table 2: Numerical boundary solution schemes used in NorShelf. All four model boundaries use the same schemes. Nudging towards the boundary TOPAZ fields is imposed within an area of 30 grid points from the boundaries with decaying nudging coefficients.

A sponge zone with increased horizontal tracer diffusivities and nonzero horizontal viscosity is implemented within 30 grid points from the boundary (see sec. 2.7). In the hindcast and forecast runs, nudging towards the boundary TOPAZ fields is imposed within the sponge zone. 2D momentum anomalies are radiated out of the model domain using the tangential phase speed of the barotropic signal, using ROMS' RADIATION_2D compiler option.

2.4 Surface forcing

Atmospheric surface fields from ECMWF's integrated forecast system are used as surface forcing in NorShelf. Archived 3-hourly fields with 0.1° resolution from the operational forecasts of the 00:00h and 12:00h reference time runs are used. The variables provided by ECMWF are given in Tab. 3, along with the respective fields required as input for ROMS.

ECMWF variables	ROMS input fields
wind at 10m height	wind at 10m height
air temperature at 2m height	air temperature at 2m height
dewpoint	relative humidity
surface pressure	surface pressure
accumulated rain	rain fall rate
cloud cover	cloud cover

Table 3: Atmospheric surface forcing fields used in NorShelf.

Relative humidity Q_{air} is calculated from dewpoint T_p and air temperature T_{air} according to Tetens' formula:

$$Q_{air} = 100e^{17.502 * \left(\frac{T_p}{240.97 + T_p} - \frac{T_{air}}{240.97 + T_{air}} \right)} \quad (1)$$

The calculation of surface fluxes is done internally using ROMS' bulk flux scheme, i.e. all fluxes are computed internally based on the fields of pressure, temperature, relative humidity, wind, cloud cover and rain fall rate. Short- and longwave radiation fluxes are based on the cloud cover. For the penetration depth of solar radiation, the ROMS water type 5 is chosen. The outgoing heat flux is limited to prevent further cooling of the sea surface below the freezing point, as NorShelf does not include a sea ice model.

2.5 River forcing

The river runoff in NorShelf consists of 222 river outlets along the Norwegian coast, 2 on the Swedish coast and 1 on the Scottish coast (see Fig. 4). The Norwegian river discharges are based on modeled river discharges from the Norwegian Water Resources and Energy Directorate (*Beldring et al.*, 2003), while data for the Scottish river was retrieved from the Global Runoff Data Centre (<http://www.bafg.de/GRDC>). Each river source is described in terms of a monthly climatological volume flux and a river salinity. For most rivers the salinity is set to 0. However, rivers which discharge into fjords and bays

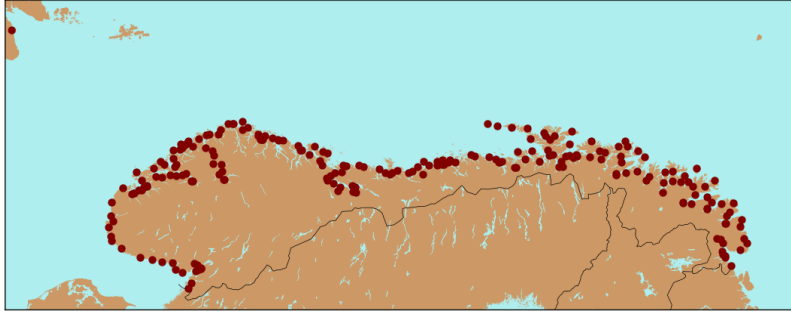


Figure 4: The 225 freshwater discharge locations in NorShelf.

unresolved by the land mask have been moved to the closest land/sea interface point (following the true coastline), and the salinity have been set to brackish values with salinities up to 18. The river inflow temperature is set equal to the ambient grid temperature.

2.6 Tidal forcing

Eight tidal constituents from the TPXO global inverse barotropic model (Egbert and Erofeeva, 2002) (Tab. 4) are imposed on velocities and free surface elevation, the tidal signal is added to these during the processing of input boundary data in ROMS.

tidal constituent	K2	S2	M2	N2	K1	P1	O1	Q1
period [h]	11.96723	12	12.4206	12.65835	23.93447	24.06589	25.81934	26.86836

Table 4: Tidal constituents used for tidal forcing in NorShelf.

2.7 Subscale processes

Turbulence

Vertical mixing is modeled using a second order scheme for turbulent kinetic energy (TKE) and a generic length scale (GLS). In this setup, which has been recommended by Umlauf and Burchard (2005) and Warner *et al.* (2005), the GLS has non-physical units of $m^2/s^2 \cdot m^{-0.67}$. Parameters for the turbulence scheme are documented Tab. 5. It is noted that turbulence dissipation rate and turbulent length scale may be calculated from TKE and GLS according to eqs. (14) and (15) in Warner *et al.* (2005). The CANUTO_A stability function is chosen for the diffusion of momentum and tracers (Canuto *et al.*, 2001; Warner *et al.*, 2005).

P	M	N	Kmin	Pmin	CMU0*	C1	C2	C3M*	C3P	SIGK	SIGP
2.0	1.0	-0.67	$7.6 \cdot 10^{-6}$	$1.0 \cdot 10^{-12}$	0.527	1.0	1.22	0.05	1.0	0.8	1.07

Table 5: Parameters for the GLS turbulence scheme used in NorShelf. *) parameters associated with the choice of stability function, which is set using the CANUTO_A compiler option.

The boundary condition for TKE at the surface is based on the model of Craig and

Banner (1994) using a flux condition, wherein the energy flux at the surface is proportional to the air-side friction velocity with a factor of 100. Surface roughness is set by the wind stress using a Charnock constant of 1400. Buoyancy and shear are horizontally smoothed using the N2S2_H0RAVG compiler option. The background vertical diffusivity is set to $10^{-6}\text{m}^2/\text{s}$ for tracers, $10^{-5}\text{m}^2/\text{s}$ for momentum and $5 * 10^{-6}\text{m}^2/\text{s}$ for TKE and GLS. Furthermore, the compiler options RI_SPLINES, SPLINES_VVISC and SPLINES_VDIFF are turned on.

Horizontal diffusion

Harmonic horizontal diffusion of tracers is applied using a diffusivity of $10\text{m}^2/\text{s}$ in the 4D-Var setup and $2\text{m}^2/\text{s}$ in the free run. Towards the boundaries, the diffusivity is increased 50-fold within a distance of 30 grid points using an arctangent shaped smooth transition (Fig. 2d). The higher diffusivities in the 4D-Var setup are required to remove strong gradients at the boundary which result from the clamped boundary conditions in the 4D-Var setup.

Explicit harmonic horizontal diffusion of momentum is applied only in the sponge zone of 30 grid points, increasing from zero to a viscosity of $100\text{m}^2/\text{s}$ using an arctangent shaped smooth transition (Fig. 2d). A harmonic horizontal diffusivity for TKE and GLS is set to $0.1\text{m}^2/\text{s}$.

Tracers are mixed along surfaces of constant geopotential, while momentum is mixed along the bottom topography following coordinate surfaces.

Bottom drag

Quadratic bottom friction is applied using a drag coefficient of 0.003 where the water depth is greater than 100m. In shallower regions, the bottom drag coefficient is increased up to 0.009 for the shallowest parts with a water depth of 10 m with linear transition as a function of water depth.

The bottom drag is limited such that the current cannot reverse sign using the pre-compiler option LIMIT_BSTRESS in ROMS. This limit is also applied in the 4D-Var setup. Limiting the bottom drag in such fashion is necessary to avoid blow-ups in the shallowest parts during strong storm surges.

2.8 Time stepping and advection schemes

NorShelf uses 120 second outer time steps for the solution of 3D momentum equations, and 3 second inner time steps for the solution of 2D momentum to resolve fast barotropic modes such as tides. During a few of the reanalysis assimilation cycles, the outer/inner time step had to be reduced to 60/1.5 seconds to avoid blow ups of the adjoint model.

Momentum and tracers are advected using a 3rd order upwind scheme in the horizontal and a 4th order centered scheme in the vertical. Turbulent kinetic energy and length scale are advected vertically and horizontally using a 4th order centered scheme.

4th order Akima advection schemes for tracers and momentum have been tested for horizontal and vertical mixing, however, this scheme introduced strong $2\Delta x$ noise in the tracer fields that could not be removed with high values of explicit diffusion (i.e. using

50m²/s). Therefore, the 3rd order upwind scheme has been chosen for horizontal tracer advection in NorShelf.

3 The NorShelf reanalysis

A reanalysis for the year 2011 has been performed using the NorShelf model, with subsequent years currently in progress. The reanalysis is initialized from a free run spin-up for 2010, whereby the spin-up was initialized with TOPAZ fields. A free control run, hereafter referred to as hindcast, for the years 2011-2012 is also performed for comparison with the reanalysis.

3.1 Observations

In-situ observations of salinity and temperature were collected from The Copernicus Marine Environment Monitoring Service (see <http://marine.copernicus.eu>), and consist of observations from a variety of observational platforms, such as monitoring cruises, FerryBox, moorings, ARGO floats, and drifting buoys. In addition to in-situ observations, SST from satellite is also used for assimilation. The SST product used in both the reanalysis and the operational suite is based on observations from infrared sensors, and consist of data from individual satellite overpasses projected onto a grid with 1.5km resolution (*Eastwood, 2011*). As clouds prevent infrared retrieval of SST, data are only available during cloud free conditions.

The observations are processed using the python toolbox `pyromsobs` (<https://github.com/metno/pyromsobs>). When more than one observation of a given state variable is available within the same grid cell at the same time, they are replaced with a so-called super-observation, which is a mean of the available observations.

3.2 The 4D-Var setup

ROMS provides several formulations of 4D-Var (*Moore et al., 2011*), of which the physical space analysis system (PSAS) is used in NorShelf. During 4D-Var, an analysis increment that minimizes a cost function based on observations and a prior background model state is calculated. The cost function consists of two terms, one that accounts for the deviation of the analysis from the observations, and one that accounts for deviations of the analysis from the prior model background state. In PSAS, the search for the best analysis increment is performed in observation space. In ROMS 4D-Var it is possible to extend the control variable vector to include surface fluxes, wind stress, and the lateral boundary conditions, in addition to the initial conditions of the ROMS state variables. This has been done for the NorShelf reanalysis. Model errors are not taken into account, i.e. PSAS is configured as strong-constraint 4D-Var.

Analysis window

The prior background state and the analysis increment along with the observations are evaluated for the duration of an analysis window such that the information in the obser-

vations is propagated in time, space, and across model variables.

In the setup chosen for the NorShelf reanalysis, the assimilation window is two days. This choice is based on the experience from previous 4D-Var experiments on the coast off Norway with 2.4km resolution (*Sperrevik et al.*, 2015, 2017). In a nutshell, a long assimilation window is desired to propagate the information by the observations as far as possible, while a limit on the window length is imposed by assuming that model physics may be linearized, as is done during 4D-Var.

Inner/outer loops

In 4D-Var, the search for an analysis increment that minimizes the cost function involves looping over forward- and backward integrations of the tangent linear and adjoint models, respectively. During these loops, termed inner loops, the gradient of the cost function is used to calculate the size and direction of an increment that will render a lower value of the cost function. The model state during the analysis window is thereby linearized around a model trajectory of full non-linear model physics. This procedure may be repeated by introducing so-called outer loops, where the model trajectory is re-linearized by performing another integration of the nonlinear model, while taking the intermediate analysis increments from the inner loops into account. In the NorShelf reanalysis, one outer loop and 12 inner loops are chosen based on sensitivity tests on the number of inner/outer loops.

Using more than 12 outer loops results in overfitting of the analysis to observations, while fewer inner loops result in poor convergence of the linear cost function. Using two outer loops instead of one did not result in a significant reduction of the final cost function, and has been described as not efficient for PSAS (A. Moore, pers. communication 2017).

Decorrelation scales

In 4D-Var, the spatial extent of the impact of observations on the analysis increments are described using decorrelation scales for the respective variables. These are given in tab. 6, separately for vertical and horizontal scales.

	initial condition	boundary conditions	surface forcing
surface elevation	10km / 30m	100km / 30m	
momentum	10km / 30m	100km / 30m	100km
tracers	10km / 30m	400km / 120m	100km

Table 6: Horizontal/vertical decorrelation scales for error covariances. For the surface forcing, the scales refer to the momentum fluxes and tracer fluxes, respectively.

4 The operational forecast suite

The operational forecast suite of NorShelf consists of a daily analysis run and a free forecast run.

An analysis model run is started each morning at 08:00 UTC. During this analysis window, the previous days (from 00:00h two days before to 00:00h of the present day)

are simulated, i.e. the analysis is 11 hours old when it is finished. Some time lag is necessary because most of the in-situ observations become available only after about one day. The forecast run is initialized from the last time step of the analysis window and integrates 5 days forward in time, i.e. about 4.5 days into the future. The analysis is initialized from the center time step of the previous analysis, such that two subsequent assimilation cycles overlap by 50%.

The computation of the analysis takes about 2.5 hours, and the forecast about 15 minutes. If the analysis does not succeed for any reason, the forecast is initialized with the model state of the 24h-forecast from the previous day. If the forecast of the previous day is lacking as well, the model is resumed from forecasts of the previous days (up to four days) to allow continuation of the operational model.

The atmospheric forcing in the analysis and forecast is based on hourly forecasts of the ECMWF, and boundary conditions are retrieved from TOPAZ forecasts provided by CMEMS (<http://marine.copernicus.eu>).

4.1 Observations

The operational analysis uses the same observation sources as the reanalysis described in sec. 3.1, but in practice the amount of in-situ observations is substantially smaller because not all observations are online available within 7-48 hours after measurement.

4.2 The 4D-Var setup

The analysis run is configured mostly identical to the NorShelf reanalysis, but with an additional requirement to save supercomputing resources, i.e. the analysis should be computed within a walltime of 2.5 hours. To facilitate this requirement, the number of inner loops are limited to 10 and adjustment of boundary conditions and surface fluxes are turned off in the PSAS algorithm, i.e. only initial conditions are adjusted. These requirements may be relaxed during further development of the model system.

5 Examples

Examples of the NorShelf reanalysis and operational analysis are presented in this section. Surface fields and vertical sections of the model hydrography are shown, as well as diagnostics of the 4D-var assimilation system.

5.1 Reanalysis

Surface fields

Instantaneous temperature and salinity fields are shown in Fig. 5 and 6 for March 1 2011 and October 1 2011, respectively. The NorShelf surface fields are plotted on top of TOPAZ surface fields that are used as boundary condition. The NorShelf model shows a distinct separation between cold and fresh water along the coast and warmer saline water further offshore. While some minor discrepancies between the models at the NorShelf boundary may be attributed to the difference in model resolution, two major discrepancies

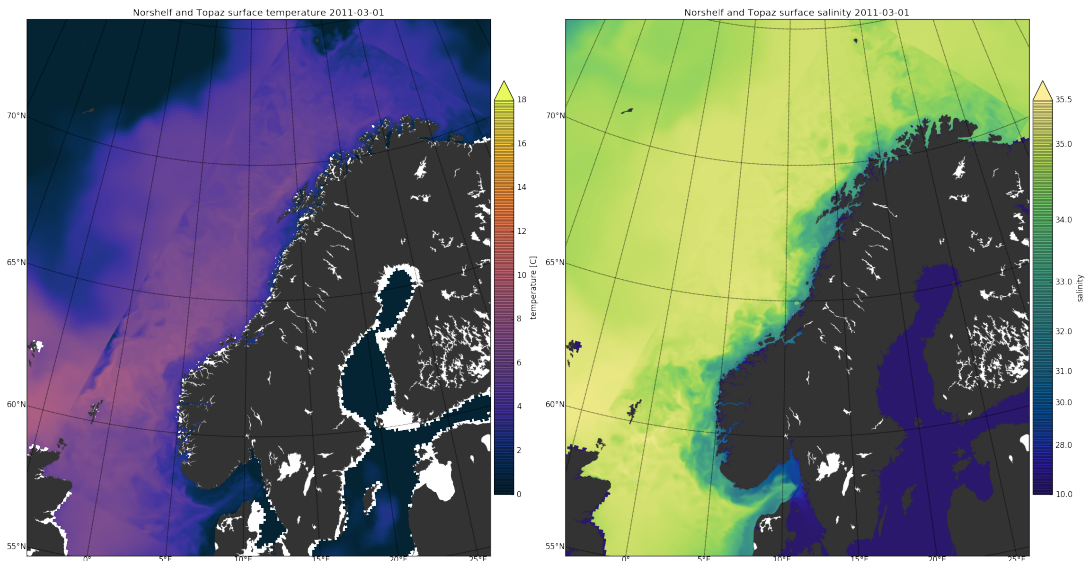


Figure 5: NorShelf surface fields of temperature and salinity, plotted on top of Topaz surface fields. Fields are daily averages from March 1st 2011.

are the result of non-resolved physics in the outer model:

First, the inflow of the North Atlantic Current north of Scotland is narrower in the NorShelf model, with sharper fronts. While TOPAZ does not resolve the sharpness of this current system, the 4D-var system in NorShelf seems to strengthen the fronts through the assimilation of SST fields. The sudden transition may also cause artifacts with too cold water near the boundary north of the inflow.

Second, the northeastern boundary in the Barents Sea has fresher water in the NorShelf model. The freshwater originates from river runoff along the coast of Norway and from the Baltic Sea, which seems to be lacking in TOPAZ. NorShelf benefits from more details in river runoff along the coast, as well as higher-resolution assimilation of observed SST fields that affect surface salinity near the coast.

Vertical sections

Model hydrography along four vertical sections is presented, along with the difference between the NorShelf reanalysis and the control run without DA. The sections are standard stations that are regularly sampled by the Institute of Marine Research. Their locations are shown in Fig. 7. In Fig. 8, model hydrography at the Torungen-Hirtshals section during March 1 and October 1 are shown. During spring, freshwater is mostly present near the coast of Norway. During autumn, a more pronounced freshwater layer is present throughout the entire section. Thermal stratification is present in both seasons but with opposite sign, i.e. cold surface water during spring and warm surface water in the autumn.

Figure 9 is for the same section as 8, showing differences between the reanalysis and the control run. Warmer and more saline water in the reanalysis are depicted as positive

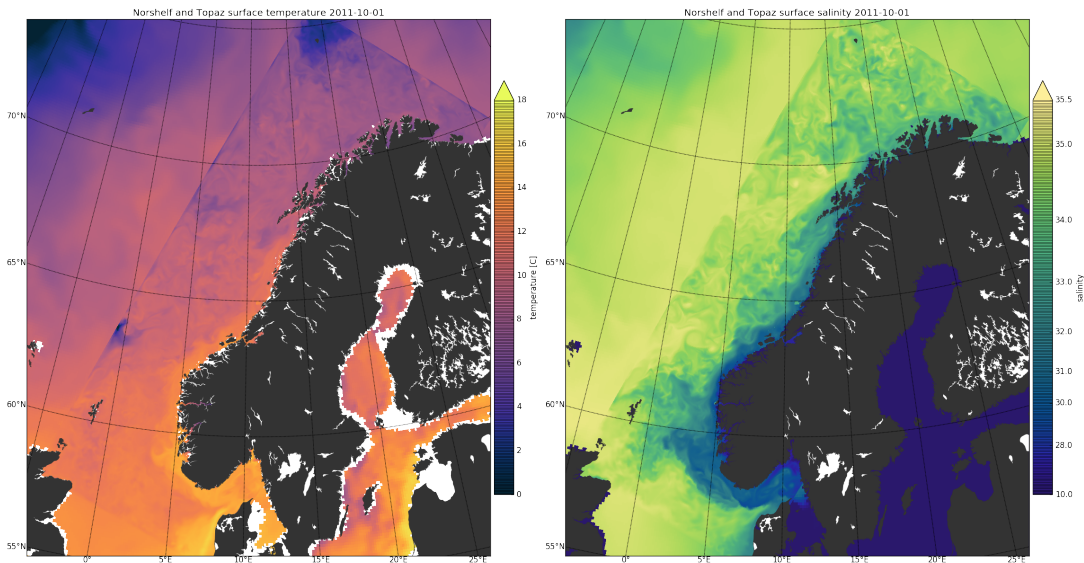


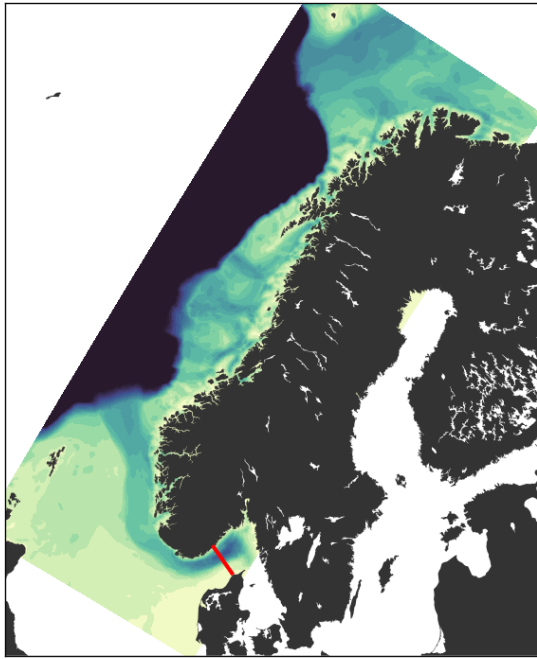
Figure 6: NorShelf surface fields of temperature and salinity, plotted on top of Topaz surface fields. Fields are daily averages from October 1st 2011.

values. In general, the assimilation system produces adjustments in model hydrography that are very different for spring and autumn, and with strong vertical and horizontal differences. Fresher coastal currents in the spring along with warmer surface water in the basin are present in the reanalysis, hence sharpening horizontal fronts and vertical stratification in the North Sea. During autumn, the entire surface layer becomes fresher. Most pronounced adjustments in temperature is a much stronger vertical stratification in the deep basin and along the coast of Norway. The surface water near the coast of Denmark becomes more sensitive to the seasonal variation in temperature.

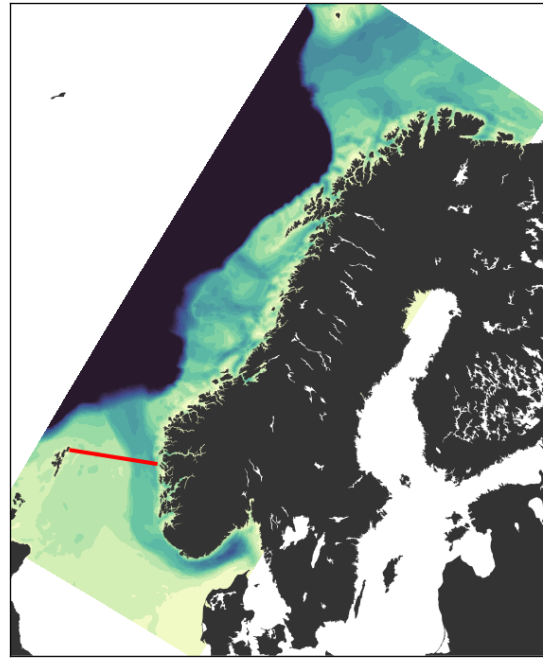
Figure 10 and 11 show model hydrography and differences at the Fedje-Shetland section off western Norway. Vertical stratification is sharpened by the assimilation system, particularly during autumn, throughout the entire section. Sharpening of vertical stratification during autumn is also a strong feature at the Gimsøy section off northern Norway (Fig. 12 and 13). At the latter section, the coastal current of fresher water on the shelf sea becomes also more pronounced in the reanalysis, both during spring and autumn. During spring, the North Atlantic current above the steep shelf slope has a more pronounced vertical structure, i.e. warm water is restricted to the surface.

Figure 14 and 15 show hydrography at the Fugløy-Bjørnøya section in the Barents Sea. As for the other sections, the vertical stratification becomes more pronounced in the reanalysis during autumn. During spring, no systematic adjustments are visible for the reanalysis, apart from some random relocation of mesoscale features. Note that no SST data as available for the assimilation system for the northernmost latitudes during winter time.

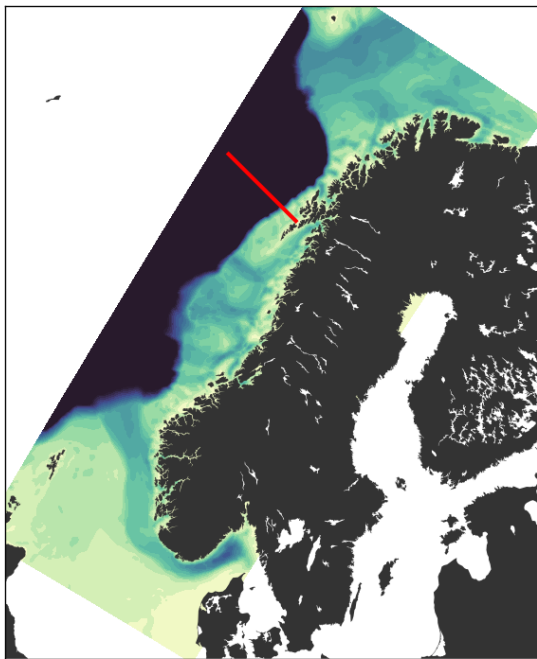
4D-var diagnostics



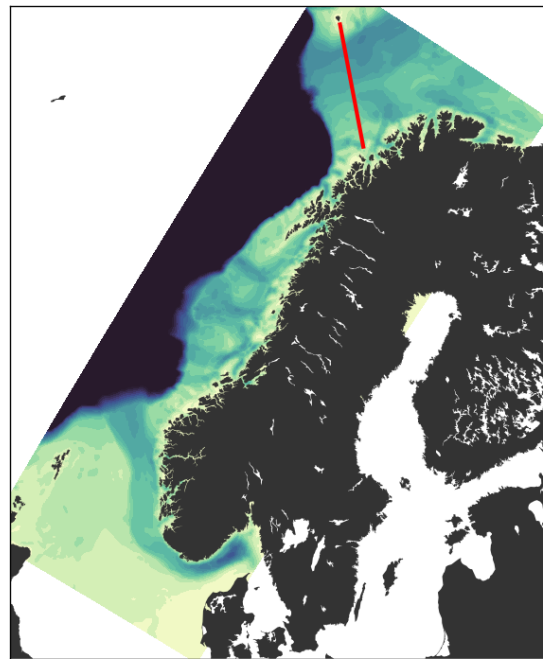
(a) Torungen-Hirtshals



(b) Fedje-Shetland



(c) Gimsoy



(d) Fugløya-Bjørnøya

Figure 7: Locations of the hydrographic sections used in Fig. 8 - 14

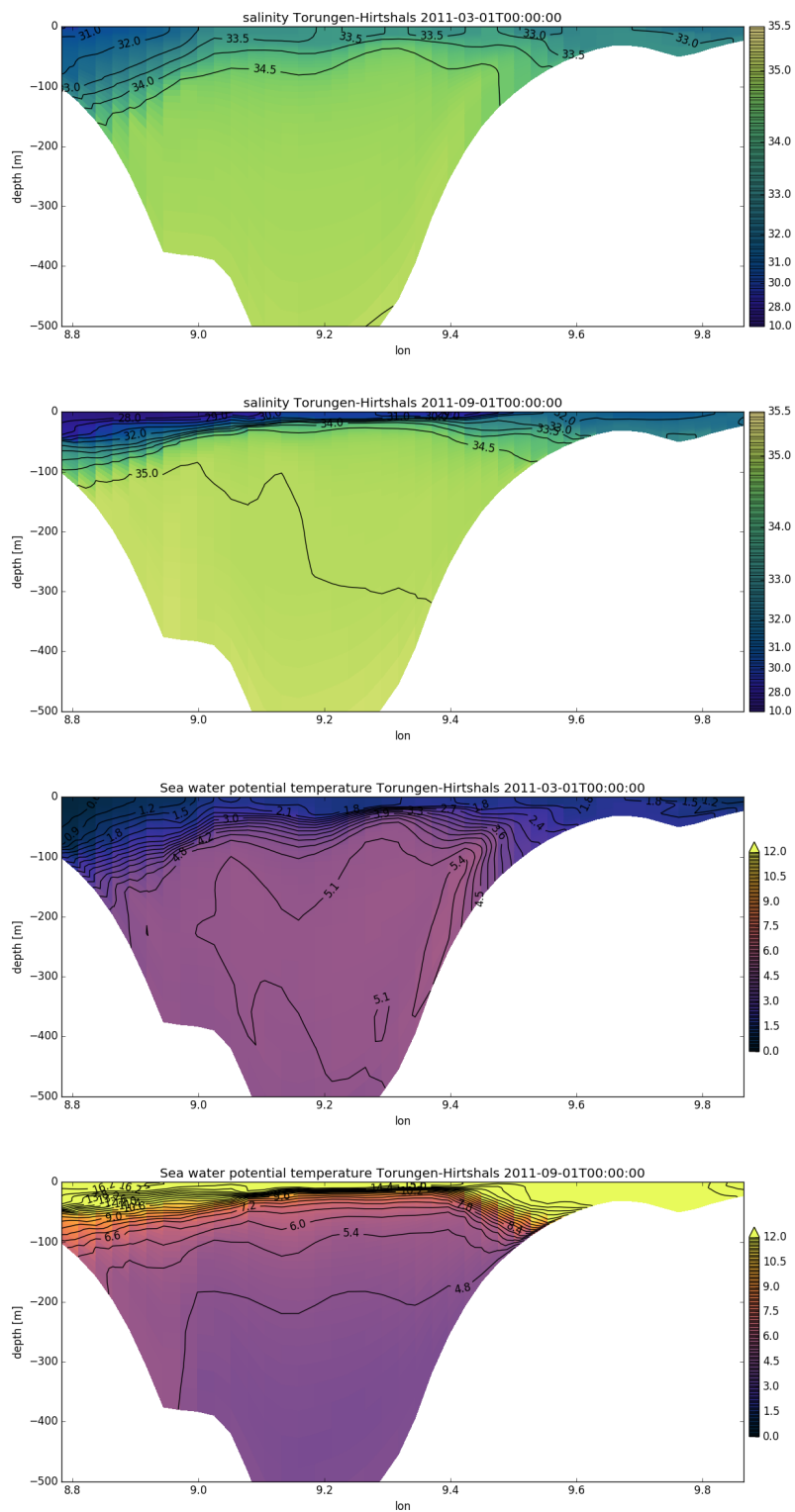


Figure 8: Vertical section of the NorShelf reanalysis at the Torungen-Hirtshals section for March 1st and October 1st 2011. The Coast of Norway (Torungen) is on the left side of this plot and the coast of Denmark (Hirtshals) on the right side.

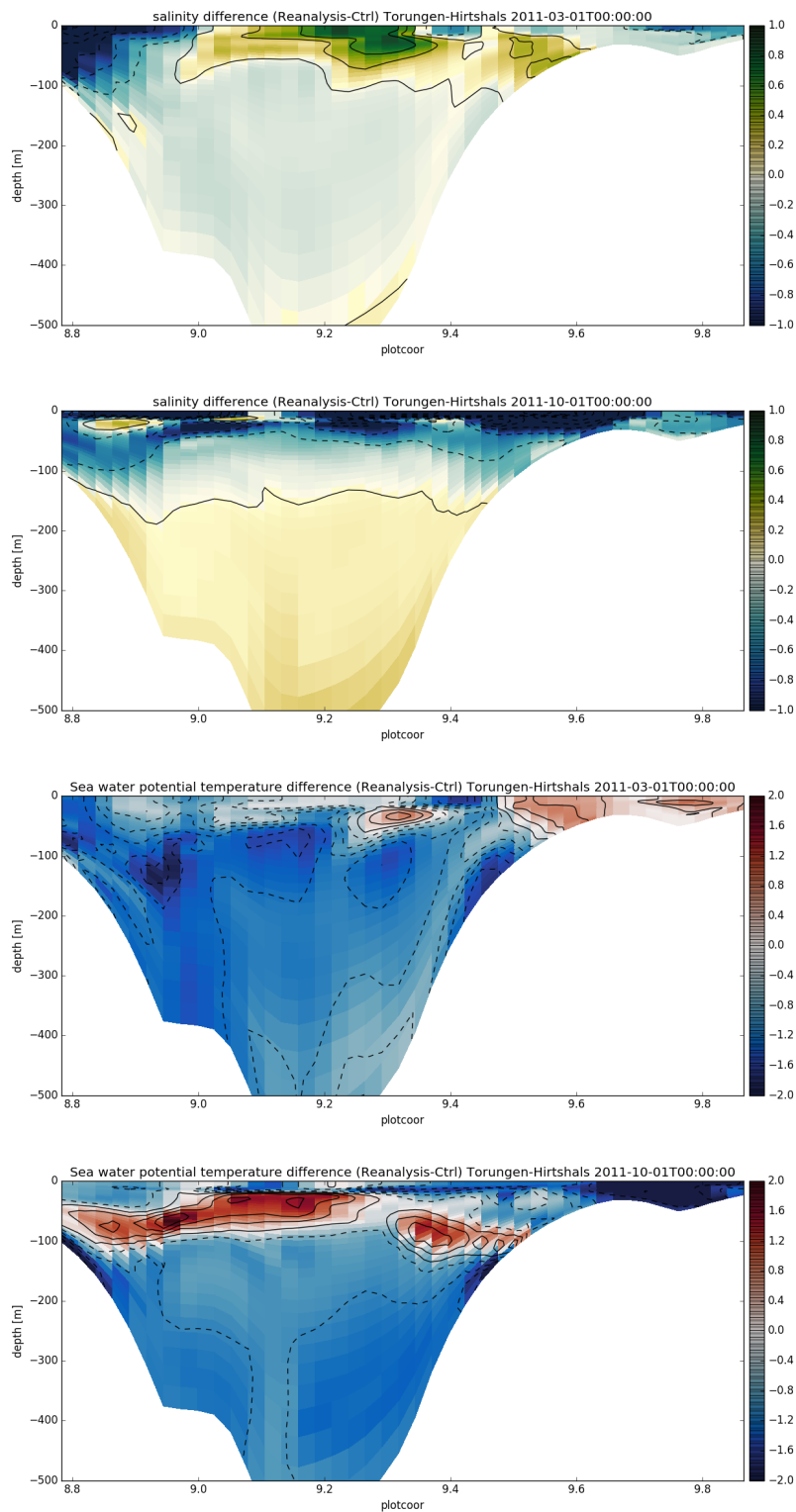


Figure 9: Difference between reanalysis and control run for the Torungen-Hirtshals section at March 1st and October 1st 2011.

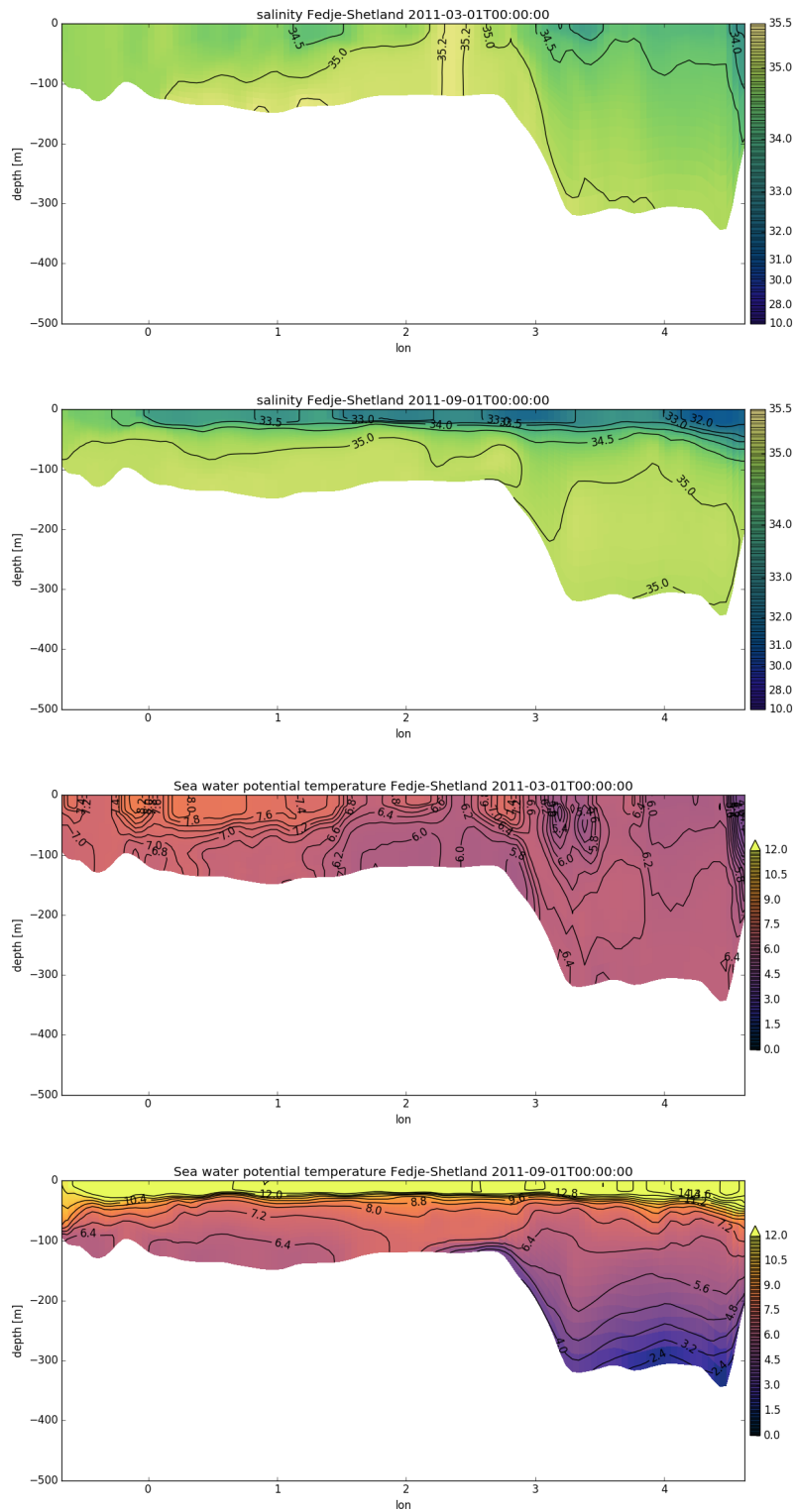


Figure 10: Vertical section at the Fedje-Shetland section for March 1st and October 1st 2011. The coast of Norway is at the right side.

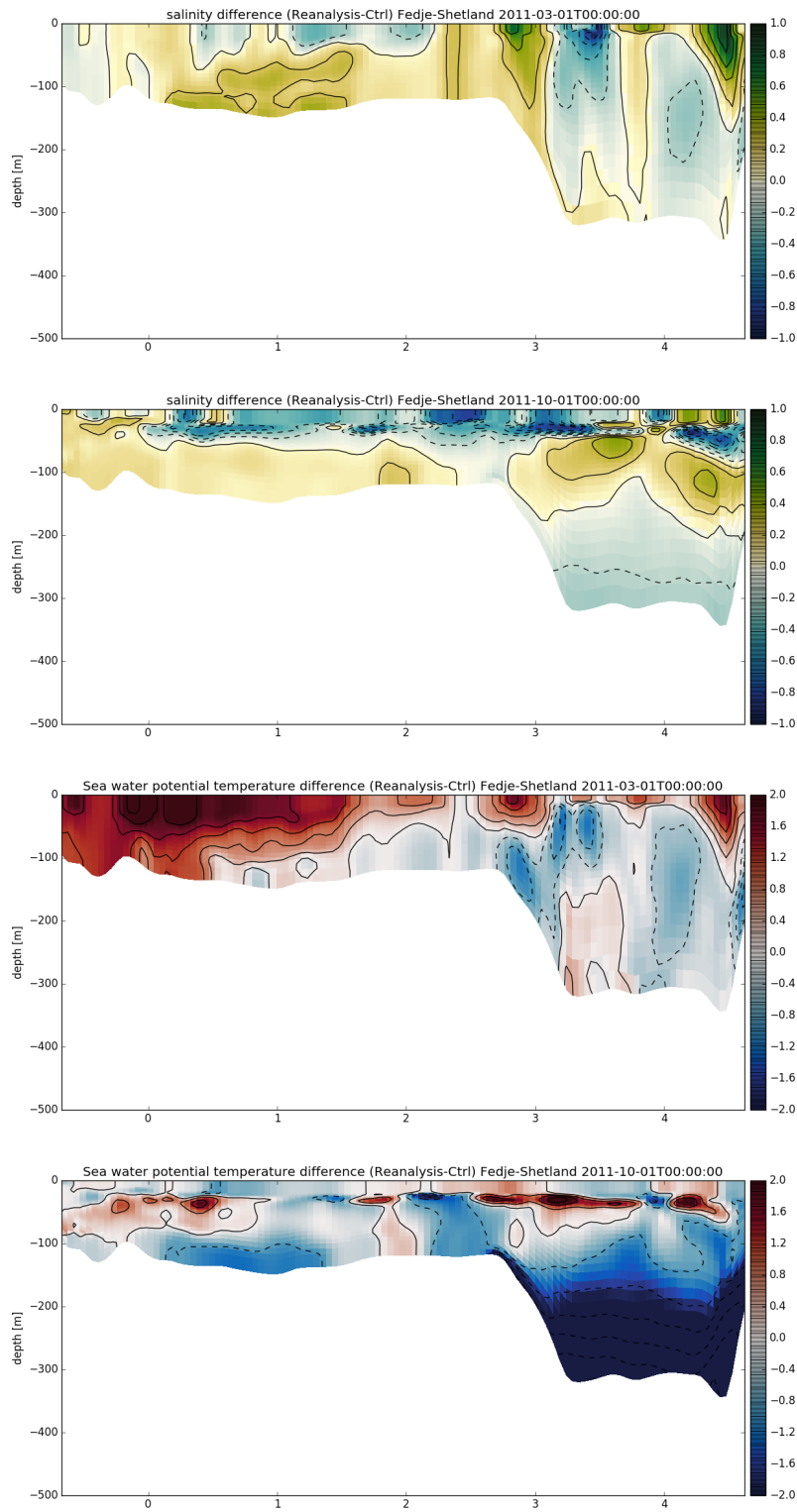


Figure 11: Difference between reanalysis and control run for the Fedje-Shetland section at March 1st and October 1st 2011.

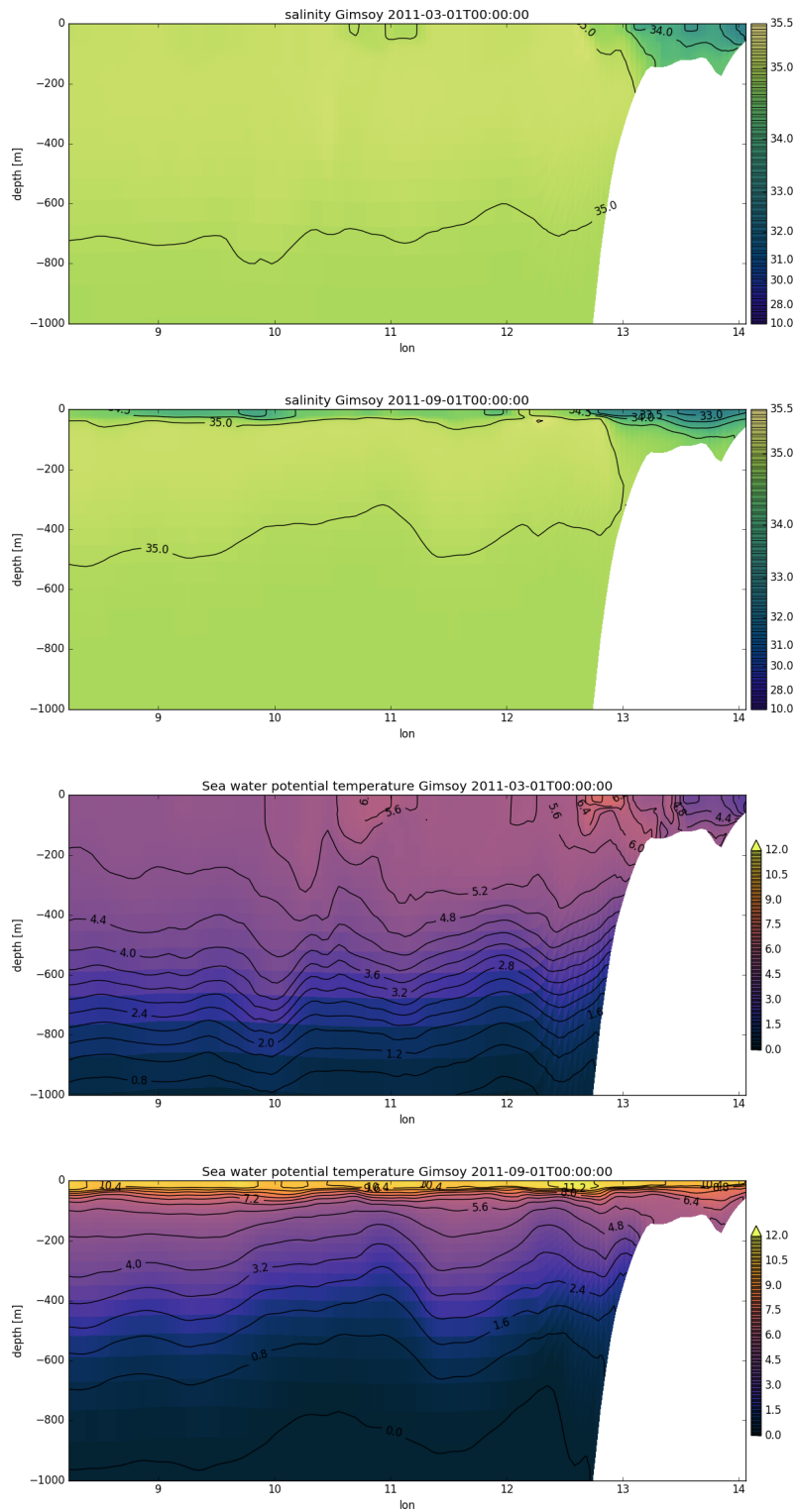


Figure 12: Vertical section at the Gimsøy section for March 1st and October 1st 2011. The coast of Norway is at the right side.

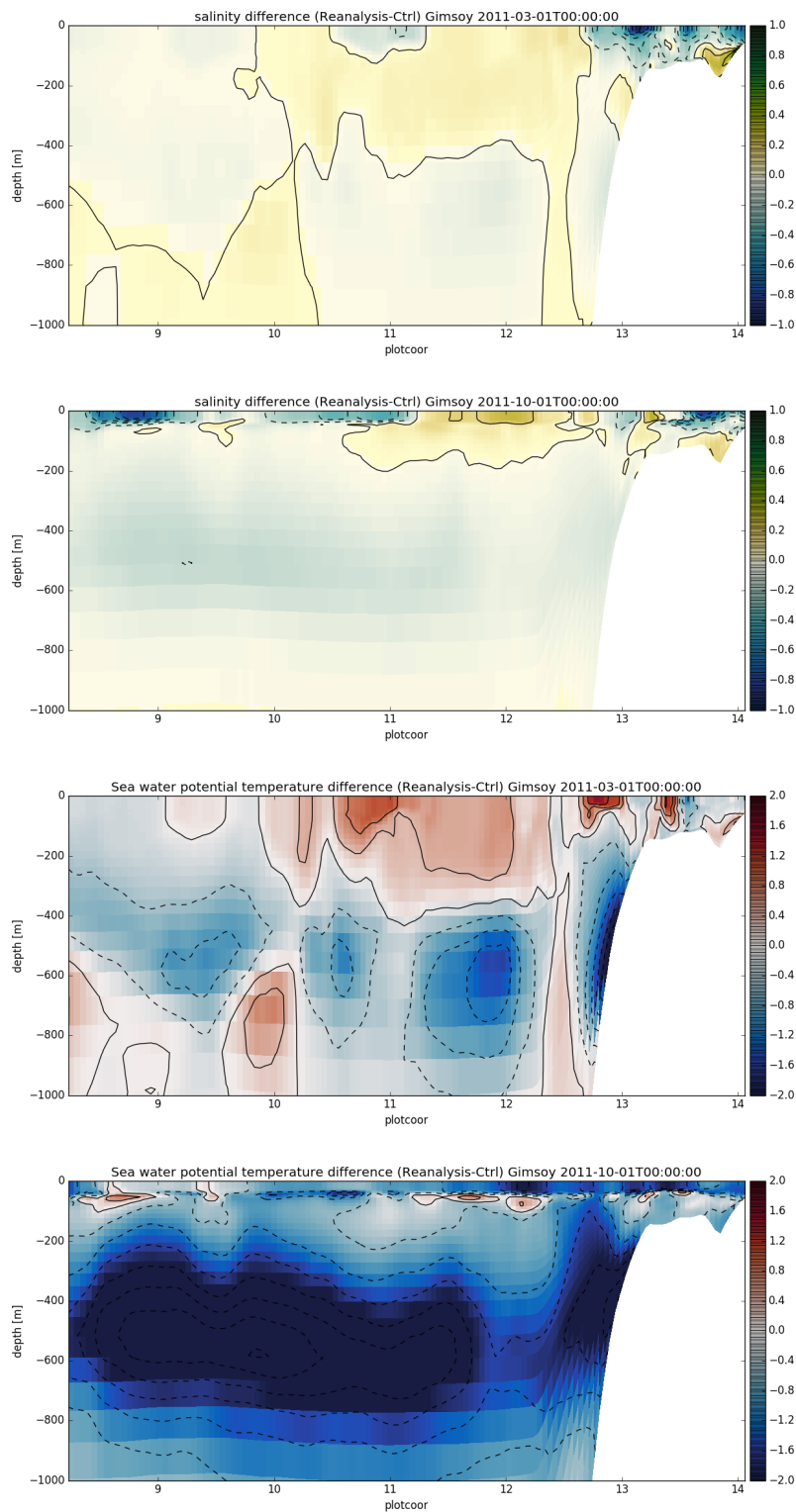


Figure 13: Difference between reanalysis and control run for the Gimsoy section at March 1st and October 1st 2011.

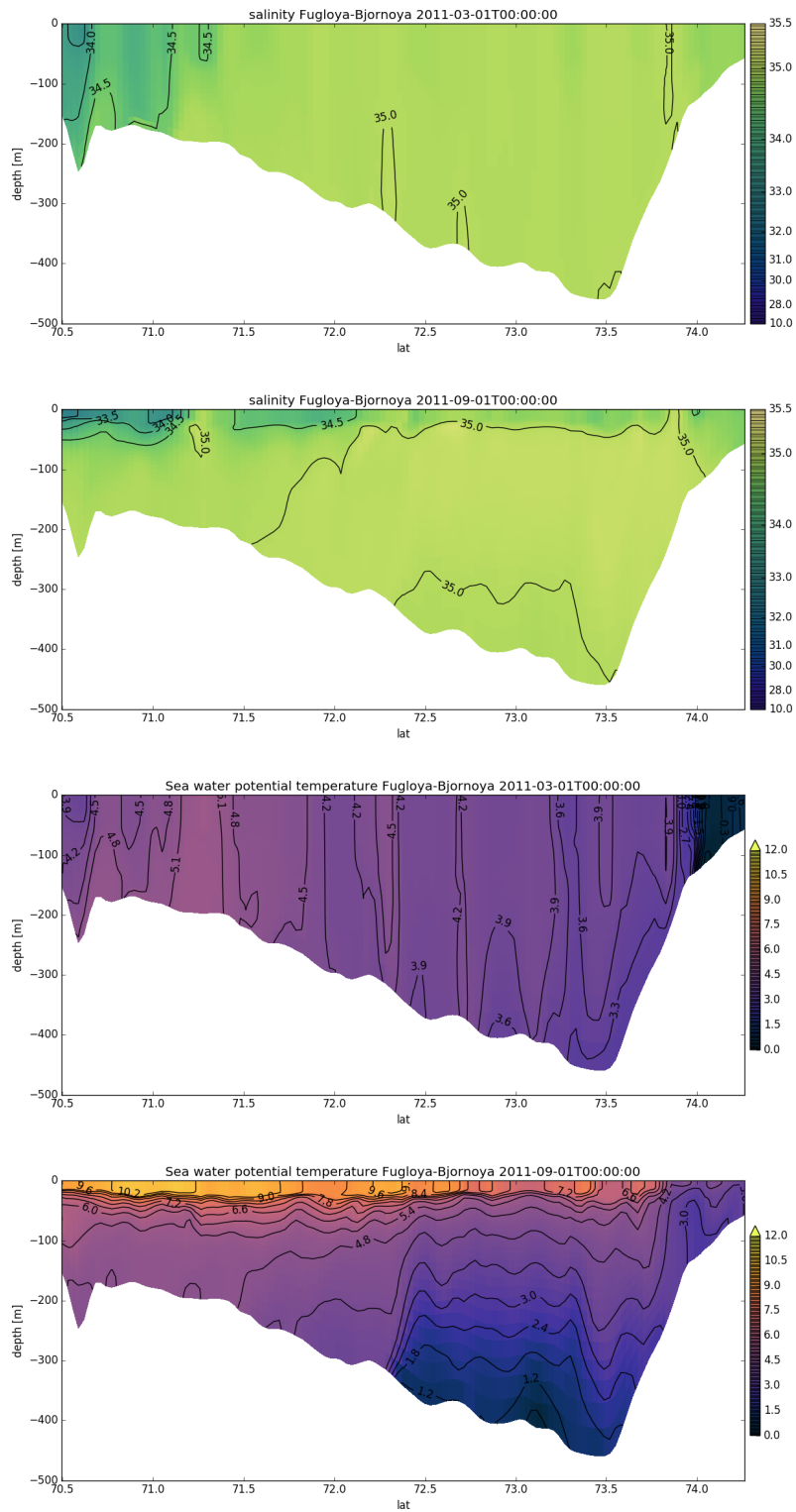


Figure 14: Vertical section at the Fugløy-Bjørnøya section for March 1st and October 1st 2011. The coast of Norway is at the left side.

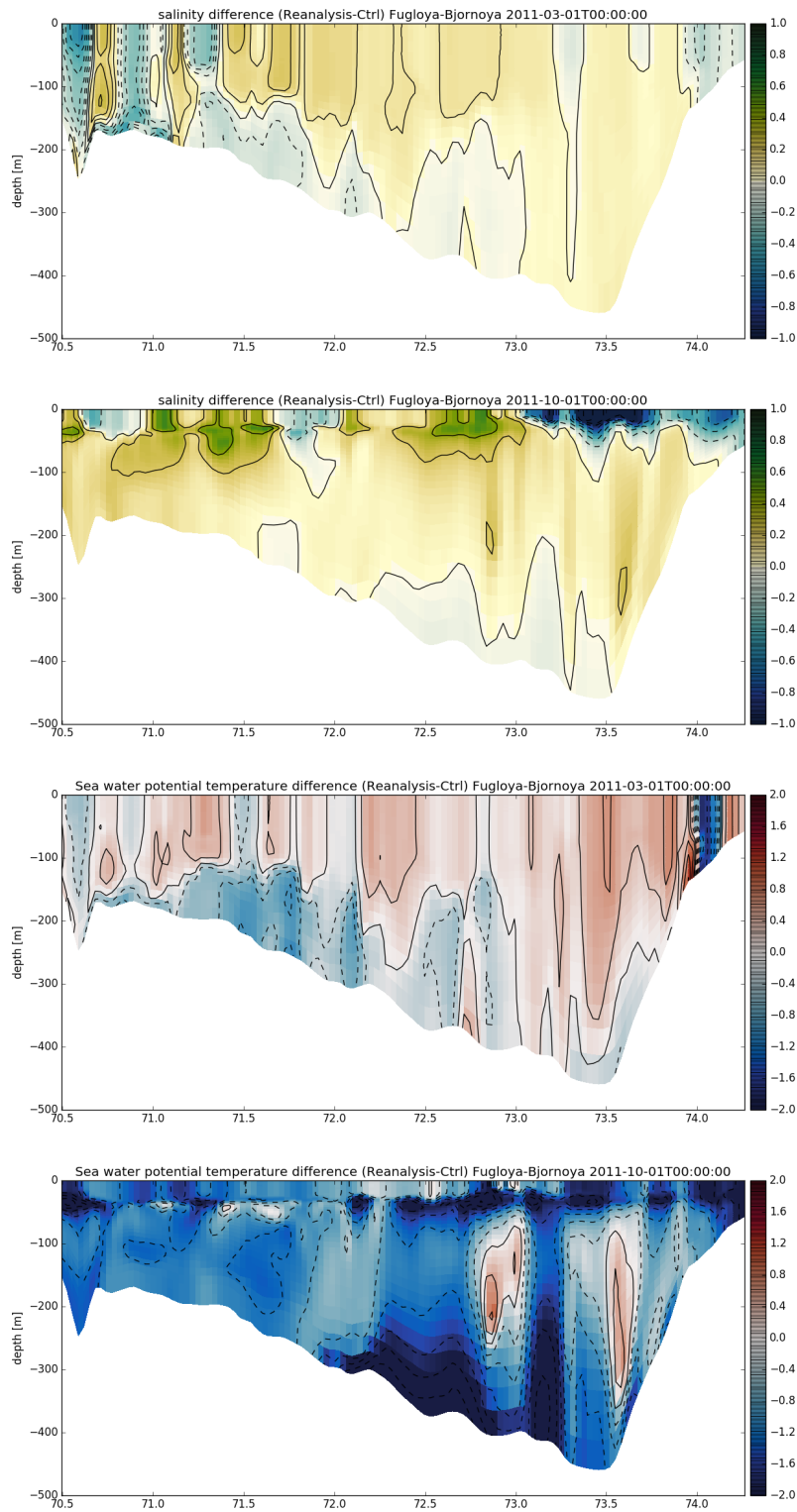


Figure 15: Difference between reanalysis and control run for the Fugløy-Bjørnøya section at March 1st and October 1st 2011.

The performance of the 4D-var system, in terms of how well it adjusts the model state to fit observations as well as to produce a posterior model state that is consistent with model physics, is discussed here with aid by Fig. 16 and Fig 17. Fig. 16 shows results of the 3rd cycle in the reanalysis, i.e. at the very beginning of the reanalysis when the model has not properly adjusted to observations and the 4D-var system. Fig. 17 shows a later cycle, after the model is well adjusted to the observations. The linear cost function (panels a) for the iterations in each cycle is expected to drop and eventually converge to a low value. Both cycles show some convergence. At the same time, the Lanczos Eigenvalues (panels b) increase during the iteration cycles, and further iteration above a value that is 100-fold the initial value is considered to be detrimental for the analysis by overfitting the model to the observations (*Moore et al.*, 2018) . A limitation to 12 inner loops in this 4D-var setup is a compromise between convergence of the cost function and keeping the Lanczos Eigenvalues below or near 100 time its initial value. A sudden increase in the Lanczos Eigenvalue is often seen during the last one or two iterations, indicating that we are pushing the limits of the 4D-var system in terms of preventing overfitting.

While the inner loops in the 4D-var system use linerized model, the posterior analysis is computed using the full non-linear model. Descrepancies between the linear and non-linear models are illustrated by the difference between the cost function of the last inner loop and the value of the cost fuction for the posterior non-linear model run, which is marked by a red diamond in Fig. 16a and Fig 17a. While a certain discrepancy is inevitable, this difference is low compared to the initial value of the cost function. A time series of the values for cost-function of the inital, final and non-linear model run is shown in Fig. 18. For a well-behaving 4D-var system, both the final and the non-linear cost function value should always be well below the inital value. This criteria is fulfilled for most cycles of the reanalysis, while a few cycles stand out with somewhat weaker results.

Fig. 16c,d and Fig 17c,d show model salinity of the prior (red) and posterior (blue) analysis, as scatter plot observed vs. modeled value. For the early cycle, an initial temperature bias is removed by the 4D-var system (Fig. 16d), and the later cycles show no more bias in the prior (e.g. 17d). In general, 4D-var reduces the scattering of model vs. observed temperature in all cycles. Salinity observations are sparse, and scatter in salinity is greatly rudedced in the posterior. The average misfit of temperature between model and observation for all cycles in the reanalysis is shown in Fig. 19. In the prior, both negative and positive descrepanices are evident for the model. During summertime, negative temperature bias is more common in the model. For the posterior, the misfit is generally lower but alwas positive during winter and always negative during summer.

5.2 Analysis and forecast

For the operational analysis, there are generally fewer observations than for the reanalysis available because many in-situ observations are beeing reported with a delay of more than 1-2 days. As an example, the number of observations for the analysis cycle on 2018-04-15 are reported in Fig. 20. Satellite SST observations are by far the most abundant. CTD and glider observations of hydrography are sparse but valuable because they provide information on the vertical structe of the density field.

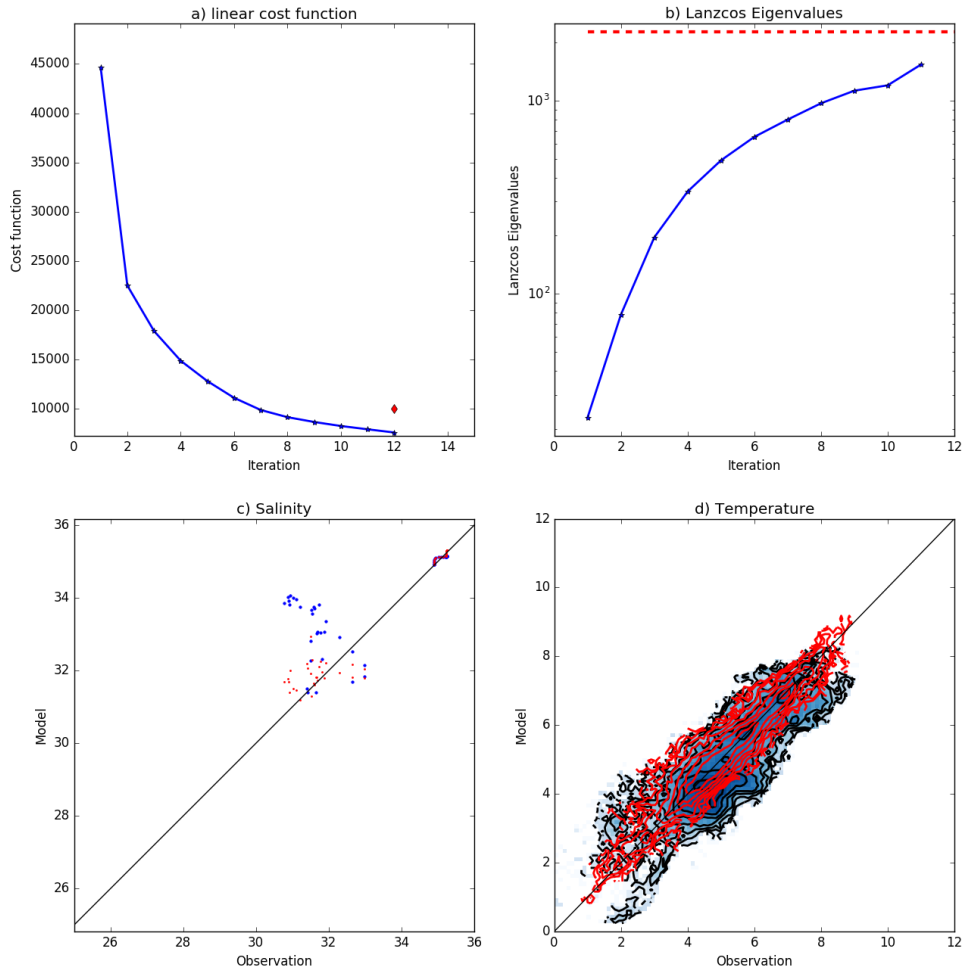


Figure 16: 4D-var diagnostics for the 3rd cycle of the NorShelf reanalysis. a) Cost function of the tangent linear model for each inner loop (blue line) and final cost function of the non-linear model. b) Lanzcos Eigenvalues, with the red dashed bar indicating a value of 100 time the initial value. c) Model salinity vs. observation for the prior (blue) and posterior (red) analysis. d) Model temperature vs. observation for the prior (blue shading and black contours) and posterior (red contours) analysis.

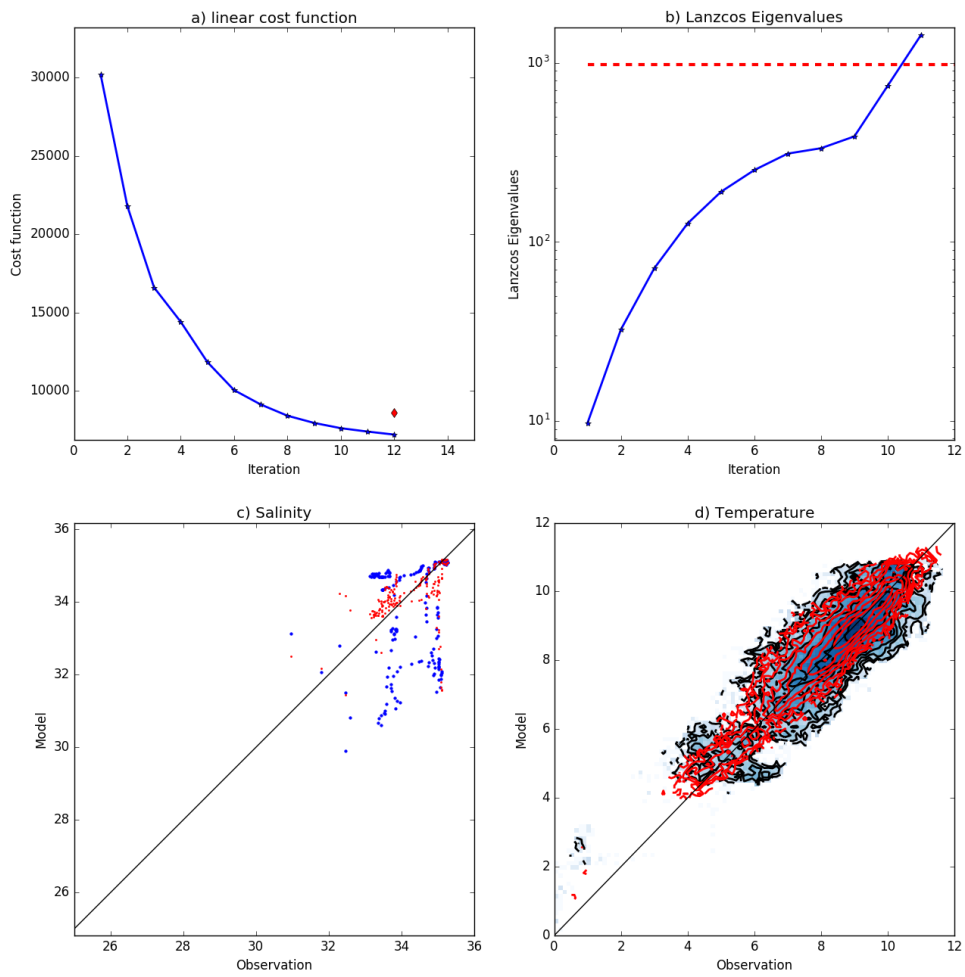


Figure 17: 4D-var diagnostics for the 164th cycle of the NorShelf reanalysis (as in Fig. 16)

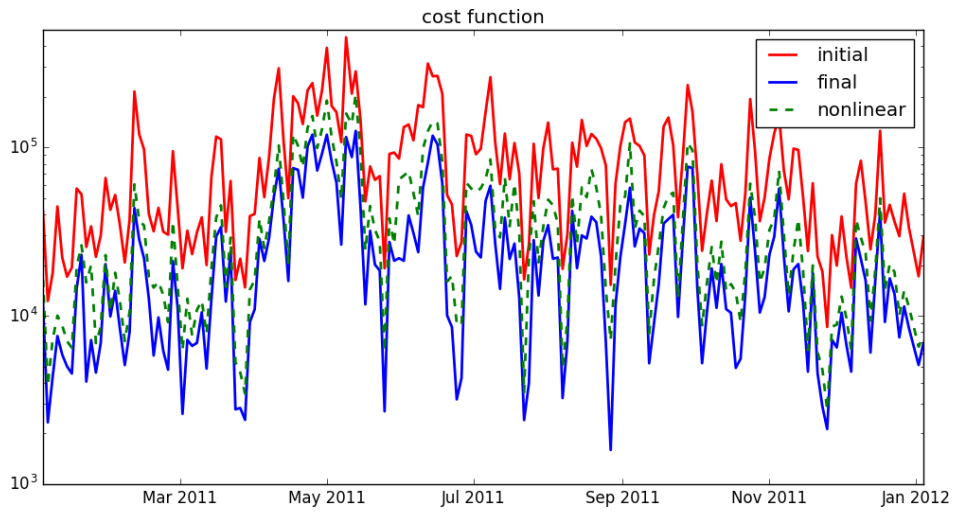


Figure 18: Value of initial linear (red), final linear (blue) and final nonlinear (dashed green) cost function for each analysis cycle in the NorShelf reanalysis

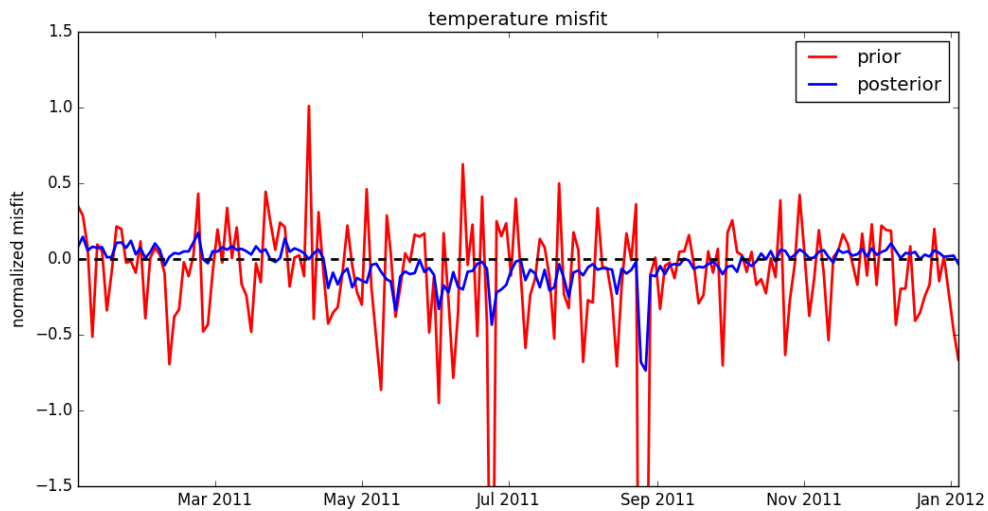


Figure 19: Average temperature misfit between observed and model value for the Nor-Shelf reanalysis, given for prior (red) and posterior (blue) model run for each reanalysis cycle

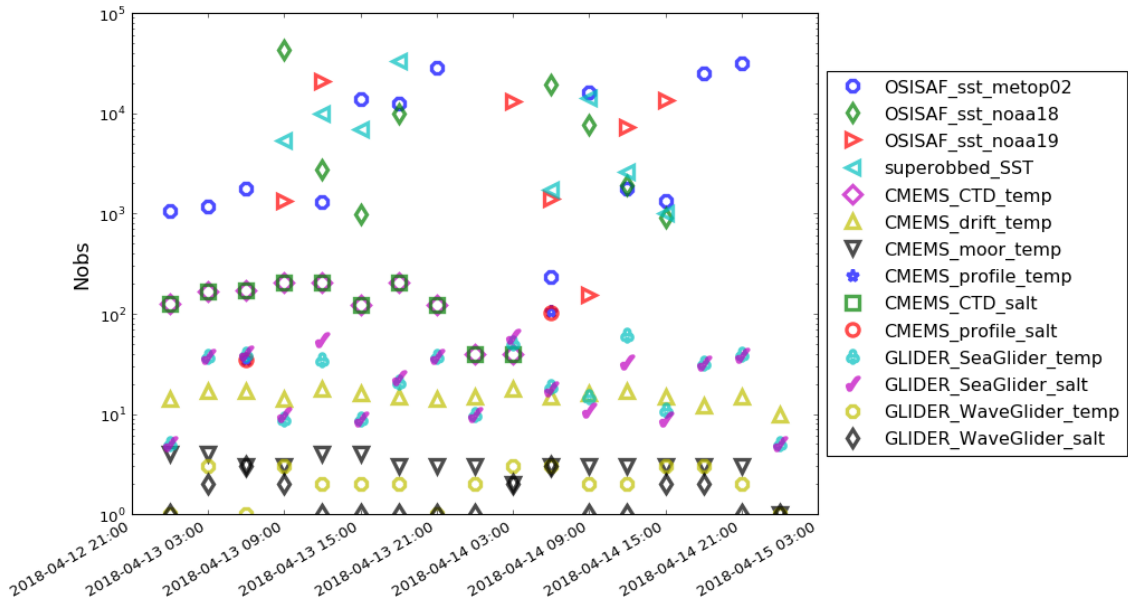


Figure 20: Number of observations available for analysis cycle on 2018-04-15.

Surface fields and analysis increments

Results for two operational analysis cycles are displayed in Fig. 21 and 23. The figures display available observations (left columns) and the resulting model SST after assimilation and the difference between the prior and posterior for temperature and salinity (right panels). During the course of one assimilation window (2 days), SST fields often cover large parts of the model domain, while the in-situ measurements only provide few points (sometimes as vertical profiles). Nevertheless, adjustments in both temperature and salinity are commonly seen over the entire model domain (lower right panels).

The dynamic response to the adjustments by the 4D-var system are illustrated for two cycles in Fig. 22 and 24. Surface currents speeds are altered throughout the entire model domain, which leads to an overall increase in eddy kinetic energy (EKE), i.e. mesoscale eddies are strengthened and possible also introduced by the 4D-var system. Changes in vorticity are both positive and negative, suggesting that the 4D-var system slightly changes the position of existing mesoscale eddies.

4D-var diagnostics

Diagnostics that evaluate the performance of the 4D-var system in the operational analysis are displayed in Figs. 25 and 25 for two cycles (compare sec. 5.1. The value of the cost function for the inner loops decay asymptotically, but convergence may be insufficient in a strict sense. Fewer inner loops are chosen than for the reanalysis to save computational costs. Overfitting to the observations is therefore rarely an issue in the analysis. For the first shown analysis cycle for 2018-04-15, a high number of in-situ observations was available (see Fig. 21), and the 4D-var system helps to reduce scatter in salinity (Fig. 25, lower left panel). However, it seems that the 4D-var system does not have the freedom to reduce scatter in temperature (lower right), possible because the majority of the temper-

NorShelf Data Assimilation System 2018-04-15

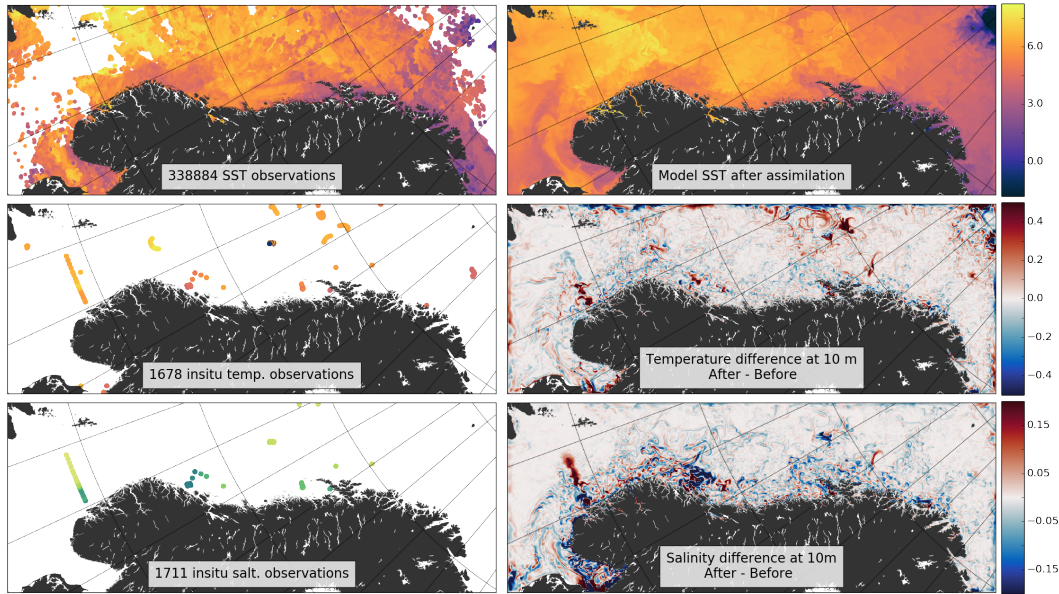


Figure 21

NorShelf Data Assimilation System Impact 2018-04-15

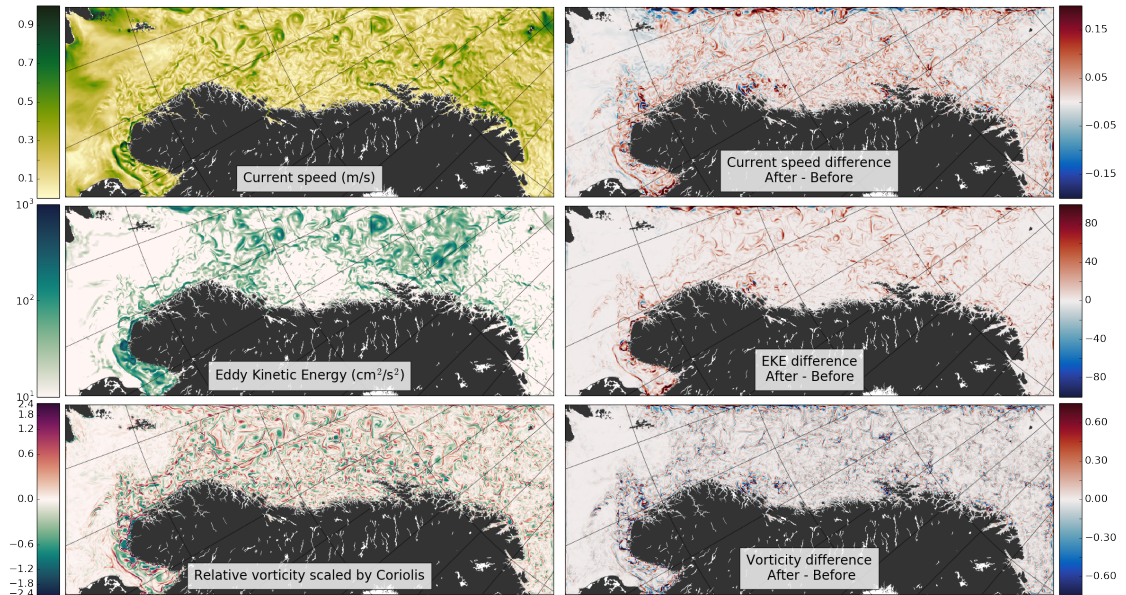


Figure 22

NorShelf Data Assimilation System 2018-04-18

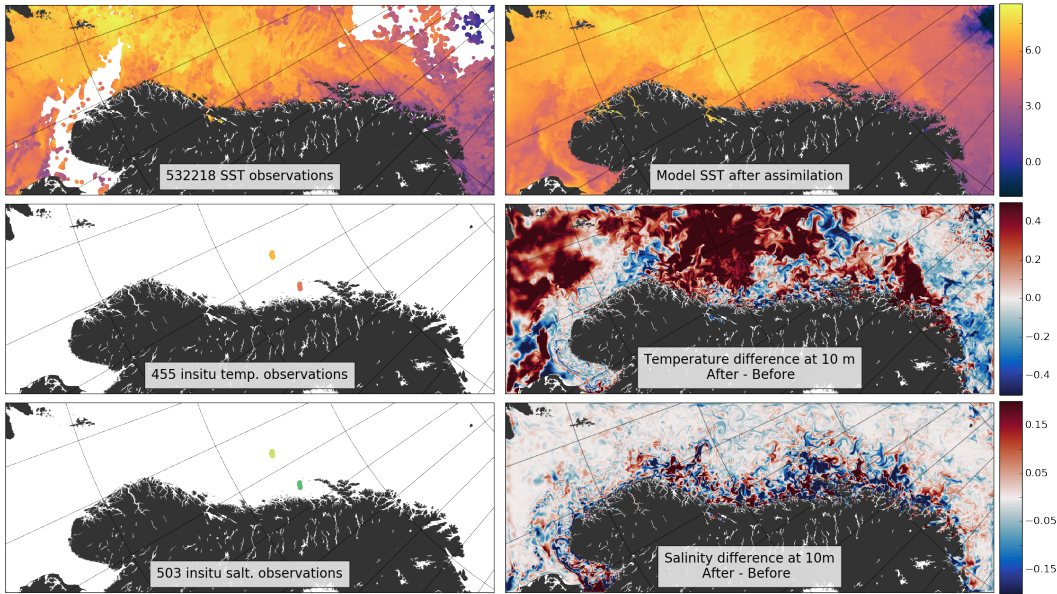


Figure 23

NorShelf Data Assimilation System Impact 2018-04-18

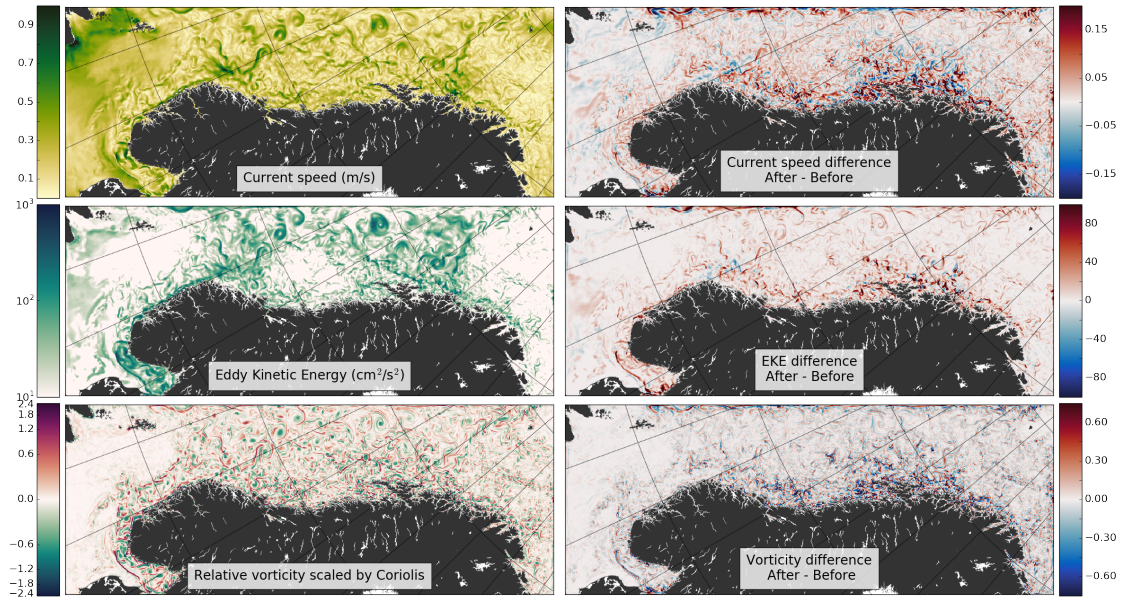


Figure 24

Table 7: Output variables available from the NorShelf forecast. In addition, the model bathymetry and grid information are available in all files.

	hourly z-grid	hourly s-grid	3-hourly s-grid	daily averages s-grid
sea surface elevation	x	x	x	x
sea water eastward velocity	x			
sea water northward velocity	x			
sea water x velocity		x	x	x
sea water y velocity		x	x	x
upward sea water velocity				x
barotropic x sea water velocity		x	x	x
barotropic y sea water velocity		x	x	x
sea water salinity	x	x	x	x
sea water temperature	x	x	x	x
turbulent generic length scale			x	
turbulent kinetic energy			x	
salinity vertical diffusion coefficient		x	x	x

ature values are from SST and with a lot of in-situ observations the model may not have the freedom to adjust surface temperature.

During the second shown analysis cycle (2018-04-18, Fig. 26), there are few in-situ observations and the scatter in temperature between observation and model is greatly reduced by the 4D-var system, in addition there was a bias in the prior that is corrected. Satellite SST observations dominate this analysis cycle. Since the NorShelf analysis has been operational, we have seen numerous cycles with significant adjustment of SST, while a few cycles stand out where a bias between SST observations and model values are present, but no bias correction is done. Typically, the bias is then corrected in a subsequent cycle (not shown).

6 Dissemination of reanalysis and forecast data

The daily NorShelf forecasts, which are initialized from the analysis cycle of each day, are available on a thredds server as an aggregated archive (<http://thredds.met.no/thredds/fou-hi/norshelf.html>). The variables and time steps that are provided on this server are summarized in Tab. 7. From the NorShelf reanalysis, both the prior and posterior model runs of each cycle are available as continuous archive (<http://thredds.met.no/thredds/retrospect.html>). A manual on how these data can be accessed is given in *Christensen et al. (2017)*.

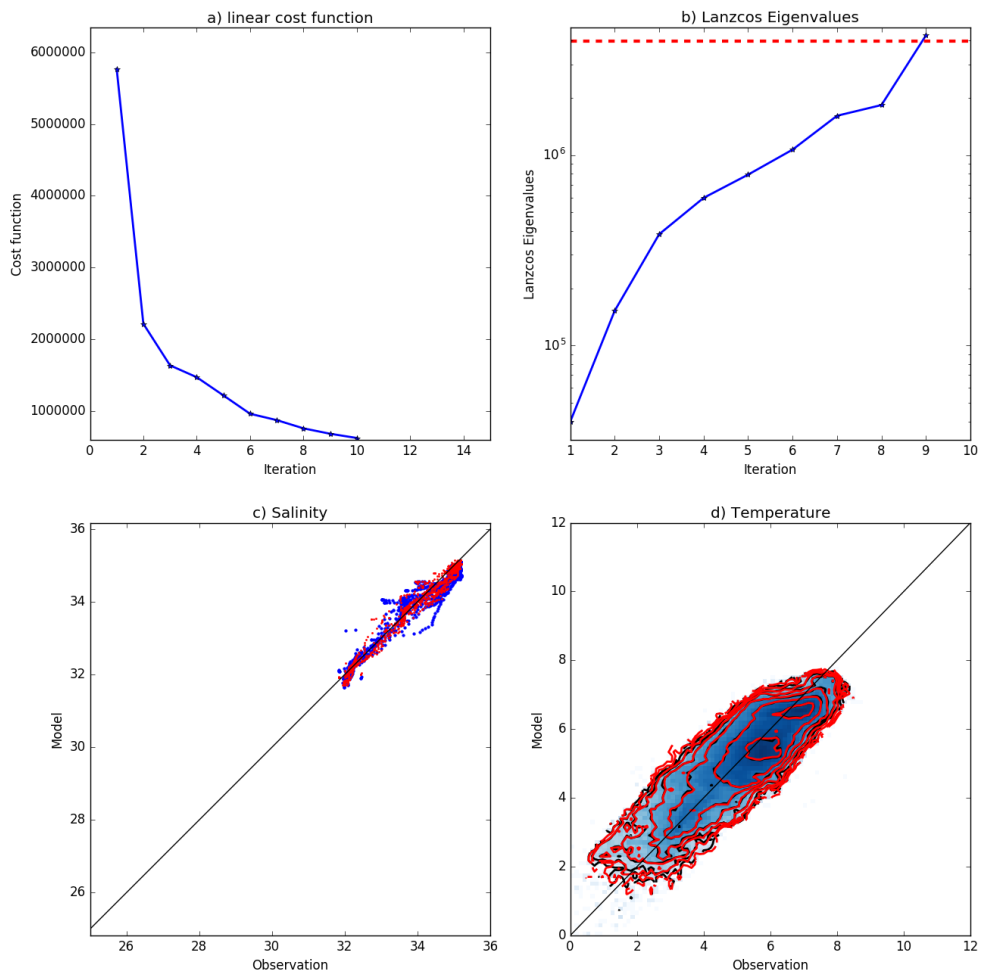


Figure 25: 4D-var diagnostics for the NorShelf analysis cycle during 2018-04-15 (as in 16)

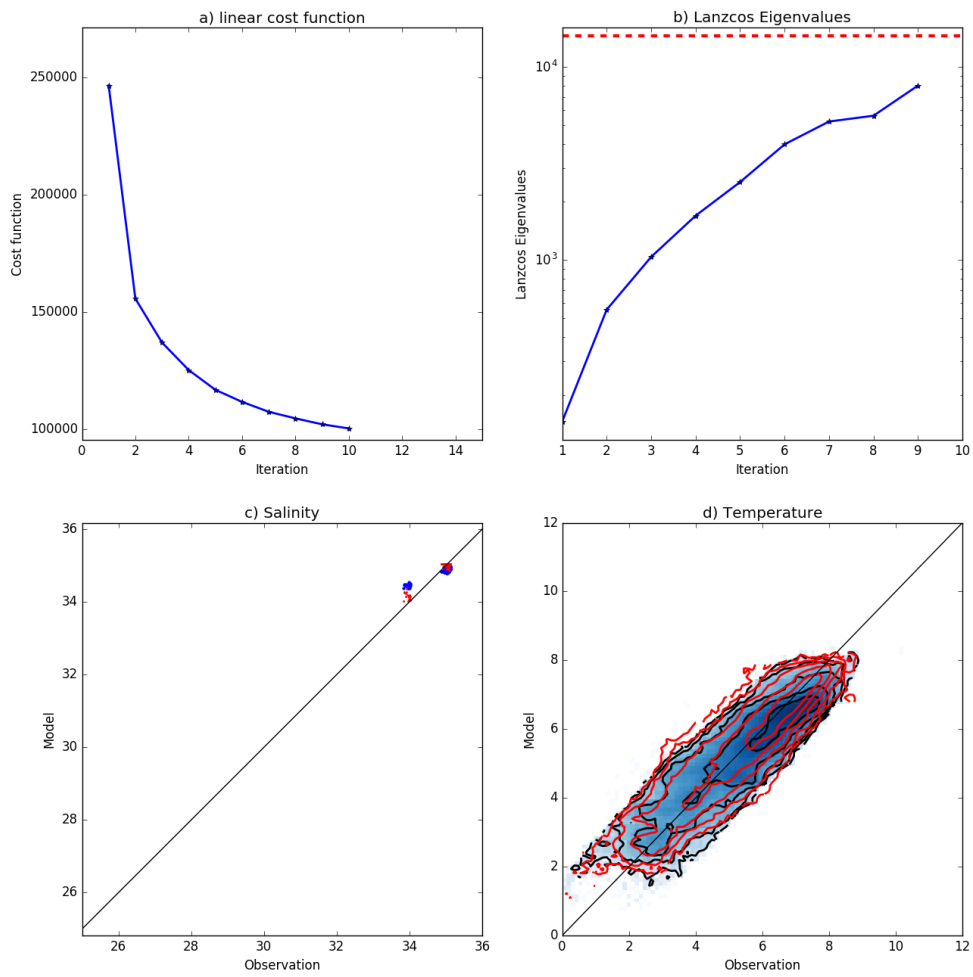


Figure 26: 4D-var diagnostics for the NorShelf analysis cycle during 2018-04-18 (as in 16)

7 Discussion and Outlook

The NorShelf model has shown to be a robust data assimilation (DA) and forecast system for the Norwegian Sea, as the model could be integrated for a year without major interruptions or development of numerical artifacts. A full year of oceanic reanalysis has been produced for 2011 and is currently being extended to include the subsequent years. In addition, the model is setup as operational ocean forecast system and has produced daily analysis and forecasts since 2017-12-01.

The main task of this model system is to perform DA, and the produced analysis are being further used within the ocean forecast systems at the Norwegian Meteorological Institute. The majority of available observations are satellite based SST fields, which cumulatively cover the majority the model domain during a 2-day assimilation cycle. Adjustments of model SST are seen as direct consequences from these data, but also surface salinity and hydrography at depth is being adjusted when only SST data is available, as seen in the hydrographic sections in Sec. 5.1.

In-situ observations of temperature and salinity are sparse, but during most assimilation cycles at least a few in-situ observations were available. Some cycles benefit locally from dense observation campaigns, e.g. when CTD sections are taken from research vessels or during glide campaigns. These types of observation have significant impact the the model trajectory, with stronger response in deeper layers compared to periods when only SST fields are assimilated. All model variables are being adjusted, and typically an increase in eddy kinetic energy is seen in the mixed layer, along with modifications to vorticity that indicate a repositioning of meso-scale eddies.

The basic criteria for a well-behaved 4D-var system are satisfied during most cycles of the NorShelf analysis and reanalysis (sec. 5.1 and 5.1). However, a few single assimilation cycles have occurred with poor performance, or where the assimilation cycle crashes with a blow-up. After such blow-ups in the operational analysis, the forecast can continue with from the forecast of the previous day instead of using the analysis as initial condition. This happens automatically, but the 4D-var system still requires some manual monitoring to keep track of such deviations, and to constantly evaluate if the 4D-var performance criteria are satisfied.

A validation of the NorShelf model against independent observation will be presented in subsequent papers. Therein, focus will be given on how well surface currents are represented by the model both statistically, as well as the skill of the forecasts in predicting surface currents. An investigation on how well the 4D-var systems improves forecasts of SST is also planned.

A technical update to the NorShelf analysis and forecast is planned for the end of 2018. The new version is going to include assimilation of surface currents from high-frequency radars and more detailed hydrography in the southeastern boundary conditions by using data from a forecast model for the Baltic Sea.

While the NorShelf model operates at an intermediate horizontal resolution of 2.4km, higher resolution models exist at MET to resolve coastal features in current patterns that are needed for coastal forecasting. The role of NorShelf in the forecast system is to perform DA at spatial scales where observations provide useful information. For the near future

it is intended that higher resolution model are nested or nudged into NorShelf to benefit from the improved hydrography and circulation that the DA in NorShelf provides.

8 Acknowledgements

The development of the NorShelf model has been financed by the Research Council of Norway through grants 244626 (RETROSPECT) and 237906 (CIRFA).

References

- Beldring, S., K. Engeland, L. A. Roald, N. R. Sva elthun, and A. Voksø (2003), Estimation of parameters in a distributed precipitation-runoff model for Norway, *Hydrol. Earth Syst. Sci.*, 7(3), 304–316, doi:10.5194/hess-7-304-2003.
- Breivik, O., A. Allen, C. Maisondieu, and M. Olagnon (2013), Advances in Search and Rescue at Sea, *Ocean Dynam.*, 63, 83–88, doi:10.1007/s10236-012-0581-1.
- Canuto, V. M., A. Howard, Y. Cheng, and M. S. Dubovikov (2001), Ocean Turbulence. Part I: One-Point Closure Model - Momentum and Heat Vertical Diffusivities, *Journal of Physical Oceanography*, 31(6), 1413–1426, doi:10.1175/1520-0485(2001)031<1413:OTPIOP>2.0.CO;2.
- Christensen, K., J. Röhrs, and A. K. Sperrevik (2017), Accessing MET Norway’s ocean model data, *MET Report ISSN 2387-4201*, Norwegian Meteorological Institute, Oslo. Report No. 23/2012, Oslo, Norway.
- Craig, P. D., and M. L. Banner (1994), Modeling Wave-Enhanced Turbulence in the Ocean Surface Layer, *Journal of Physical Oceanography*, 24(12), 2546–2559, doi:10.1175/1520-0485(1994)024<2546:MWETIT>2.0.CO;2.
- Dagestad, K.-F., J. Röhrs, O. Breivik, and B. Ådlandsvik (2018), OpenDrift v1.0: a generic framework for trajectory modelling, *Geosci. Model Dev.*, 11(4), 1405–1420, doi:10.5194/gmd-11-1405-2018.
- Eastwood, S. (2011), Atlantic High Latitude L3 Sea Surface Temperature Product User Manual, *AHL L3 SST Product User Manual*, Norwegian Meteorological Institute.
- Egbert, G. D., and S. Y. Erofeeva (2002), Efficient inverse modeling of barotropic ocean tides, *J. Atmos. Ocean. Tech.*, 19(2), 183–204, doi:10.1175/1520-0426(2002)019<0183:EIMOBO>2.0.CO;2.
- Moore, A. M., H. G. Arango, G. Broquet, C. Edwards, M. Veneziani, B. Powell, D. Foley, J. D. Doyle, D. Costa, and P. Robinson (2011), The Regional Ocean Modeling System (ROMS) 4-dimensional variational data assimilation systems: Part III – Observation impact and observation sensitivity in the California Current System, *Progress in Oceanography*, 91(1), 74–94, doi:10.1016/j.pocean.2011.05.005.

- Moore, A. M., H. G. Arango, and C. A. Edwards (2018), Reduced-Rank Array Modes of the California Current Observing System, *Journal of Geophysical Research: Oceans*, 123(1), 452–465, doi:10.1002/2017JC013172.
- Röhrs, J., K.-F. Dagestad, H. Asbjørnsen, T. Nordam, J. Skancke, C. E. Jones, and C. Brekke (2018), The effect of vertical mixing on the horizontal drift of oil spills, *Ocean Science Discussions*, pp. 1–32, doi:https://doi.org/10.5194/os-2018-100.
- Shchepetkin, A., and J. McWilliams (2005), The regional oceanic modeling system (ROMS): a split-explicit, free-surface, topography-following-coordinate oceanic model, *Ocean Model.*, 9(4), 347–404, doi:10.1029/2008JC005135.
- Sperreik, A. K., K. H. Christensen, and J. Röhrs (2015), Constraining energetic slope currents through assimilation of high-frequency radar observations, *Ocean Sci*, 11, 237–249, doi:10.5194/os-11-237-2015.
- Sperreik, A. K., J. Röhrs, and K. H. Christensen (2017), Impact of data assimilation on Eulerian versus Lagrangian estimates of upper ocean transport, *Journal of Geophysical Research: Oceans*, 122(7), 5445–5457, doi:10.1002/2016JC012640.
- Strand, K. O., S. Sundby, J. Albretsen, and F. B. Vikebø (2017), The Northeast Greenland Shelf as a Potential Habitat for the Northeast Arctic Cod, *Frontiers in Marine Science*, 4, doi:10.3389/fmars.2017.00304.
- Umlauf, L., and H. Burchard (2005), Second-order turbulence closure models for geophysical boundary layers. A review of recent work, *Continental Shelf Research*, 25(7–8), 795–827, doi:10.1016/j.csr.2004.08.004.
- Wakelin, S. L., J. T. Holt, and R. Proctor (2009), The influence of initial conditions and open boundary conditions on shelf circulation in a 3d ocean-shelf model of the North East Atlantic, *Ocean Dynamics*, 59(1), 67–81, doi:10.1007/s10236-008-0164-3.
- Warner, J. C., C. R. Sherwood, H. G. Arango, and R. P. Signell (2005), Performance of four turbulence closure models implemented using a generic length scale method, *Ocean Modelling*, 8(1–2), 81–113, doi:10.1016/j.ocemod.2003.12.003.
- Xie, J., L. Bertino, F. Counillon, K. A. Lisæter, and P. Sakov (2017), Quality assessment of the TOPAZ4 reanalysis in the Arctic over the period 1991–2013, *Ocean Sci.*, 13(1), 123–144, doi:10.5194/os-13-123-2017.

Appendix A - ROMS compiler option

The pre-compiler options in ROMS that are used for the NorShelf analysis are listed below, as reported by the ROMS executable.

ADD_FSOBC	Adding tidal elevation to processed OBC data.
ADD_M2OBC	Adding tidal currents to processed OBC data.
ADJOINT	Adjoint Model.
ADJUST_BOUNDARY	Including boundary conditions in 4DVar state estimation.
ADJUST_STFLUX	Including surface tracer flux in 4DVar state estimation.
ADJUST_WSTRESS	Including surface wind stress in 4DVar state estimation.
ALBEDO	Shortwave radiation from albedo equation.
ANA_BSFLUX	Analytical kinematic bottom salinity flux.
ANA_BTFLUX	Analytical kinematic bottom temperature flux.
ANA_SRFLUX	Analytical kinematic shortwave radiation flux.
ASSUMED_SHAPE	Using assumed-shape arrays.
ATM_PRESS	Impose atmospheric pressure onto sea surface.
BGQC	Background quality control of observations.
!BOUNDARY_ALLGATHER	Using mpi_allreduce in mp_boundary routine.
BULK_FLUXES	Surface bulk fluxes parameterization.
CANUTO_A	Canuto A-stability function formulation.
!COLLECT_ALL...	Using mpi_isend/mpi_recv in mp_collect routine.
CHARNOK	Charnok surface roughness from wind stress.
CRAIG_BANNER	Craig and Banner wave breaking surface flux.
COOL_SKIN	Surface cool skin correction.
CURVGRID	Orthogonal curvilinear grid.
DJ_GRADPS	Parabolic Splines density Jacobian (Shchepetkin, 2002).
DOUBLE_PRECISION	Double precision arithmetic.
EMINUSP	Compute Salt Flux using E-P.
FORWARD_MIXING	Read in Forward vertical mixing for Tangent/Adjoint.
FORWARD_READ	Read in Forward solution for Tangent/Adjoint.
FORWARD_WRITE	Write out Forward solution for Tangent/Adjoint.
FULL_GRID	Considering observations at interior and boundary points.
GLS_MIXING	Generic Length-Scale turbulence closure.
HDF5	Creating NetCDF-4/HDF5 format files.
IMPLICIT_VCONV	Implicit Vertical Convolution Algorithm.
LIMIT_BSTRESS	Limit bottom stress to maintain bottom velocity direction.
LIMIT_STFLX_COOLING	Suppress further cooling if SST is at freezing point.
IMPULSE	Processing Adjoint Impulse forcing.
LONGWAVE	Compute net longwave radiation internally.
MASKING	Land/Sea masking.
MIX_GEO_TS	Mixing of tracers along geopotential surfaces.
MIX_S_UV	Mixing of momentum along constant S-surfaces.
MPI	MPI distributed-memory configuration.
NL_BULK_FLUXES	Using bulk fluxes computed by nonlinear model.
NONLINEAR	Nonlinear Model.
NONLIN_EOS	Nonlinear Equation of State for seawater.
NO_LBC_ATT	Not checking NetCDF global attribute NLM_LBC during restart.
N2S2_HORAVG	Horizontal smoothing of buoyancy and shear.
OBSERVATIONS	Processing 4DVar observations.
POWER_LAW	Power-law shape time-averaging barotropic filter.
PROFILE	Time profiling activated .
K_C4ADVECTION	Fourth-order centered differences advection of TKE fields.
RADIATION_2D	Use tangential phase speed in radiation conditions.
REDUCE_ALLGATHER	Using mpi_allgather in mp_reduce routine.
RI_SPLINES	Parabolic Spline Reconstruction for Richardson Number.
RPCG	Restricted B-preconditioned Lanczos minimization.
!RST_SINGLE	Double precision fields in restart NetCDF file.
SALINITY	Using salinity.
SOLAR_SOURCE	Solar Radiation Source Term.
SOLVE3D	Solving 3D Primitive Equations.
SPLINES_VDIFF	Parabolic Spline Reconstruction for Vertical Diffusion.
SPLINES_VVISC	Parabolic Spline Reconstruction for Vertical Viscosity.
SSH_TIDES	Add tidal elevation to SSH climatology.
TANGENT	Tangent Linear Model.
TS_U3HADVECTION	Third-order upstream horizontal advection of tracers.

TS_U3HADVECTION_TL	TL/AD third-order upstream horizontal tracer advection.
TS_C4VADVECTION	Fourth-order centered vertical advection of tracers.
TS_C4VADVECTION_TL	TL/AD fourth-order centered vertical tracer advection.
TS_DIF2	Harmonic mixing of tracers.
UV_ADV	Advection of momentum.
UV_COR	Coriolis term.
UV_U3HADVECTION	Third-order upstream horizontal advection of 3D momentum.
UV_C4VADVECTION	Fourth-order centered vertical advection of momentum.
UV_DRAG_GRID	Spatially varying quadratic drag coefficient.
UV_QDRAG	Quadratic bottom stress.
UV_TIDES	Add tidal currents to 2D momentum climatologies.
UV_VIS2	Harmonic mixing of momentum.
VCONVOLUTION	Include vertical correlations in convolutions.
VERIFICATION	Process model solution at observation locations.
W4DPSAS	Weak constraint 4D-PSAS data assimilation.
WEAK_CONSTRAINT	Activated weak constraint assimilation set-up.

Appendix B - Run-time settings for ROMS

The ROMS input parameters for the analysis cycle on 2018-10-07 are listed below.

1440	ntimes	Number of timesteps for 3-D equations.
120.000	dt	Timestep size (s) for 3-D equations.
40	ndtfast	Number of timesteps for 2-D equations between each 3D timestep.
1	ERstr	Starting ensemble/perturbation run number.
1	ERend	Ending ensemble/perturbation run number.
1	Nouter	Maximum number of 4DVAR outer loop iterations.
10	Ninner	Maximum number of 4DVAR inner loop iterations.
0	nrrec	Number of restart records to read from disk.
F	LcycleRST	Switch to recycle time-records in restart file.
1440	nRST	Number of timesteps between the writing of data into restart fields.
10	ninfo	Number of timesteps between print of information to standard output.
T	ldefout	Switch to create a new output NetCDF file(s).
90	nHIS	Number of timesteps between the writing fields into history file.
0	nQCK	Number of timesteps between the writing fields into quicksave file.
F	LcycleTLM	Switch to recycle time-records in tangent file.
90	nTLM	Number of timesteps between the writing of data into tangent file.
F	LcycleADJ	Switch to recycle time-records in adjoint file.
1440	nADJ	Number of timesteps between the writing of data into adjoint file.
90	nOBC	Number of timesteps between 4DVAR adjustment of open boundaries.
90	nSFF	Number of timesteps between 4DVAR adjustment of surface forcing fields.
5.0000E+01	nl_tnu2(01)	NLM Horizontal, harmonic mixing coefficient (m ² /s) for tracer 01: temp
5.0000E+01	ad_tnu2(01)	ADM Horizontal, harmonic mixing coefficient (m ² /s) for tracer 01: temp
5.0000E+01	tl_tnu2(01)	TLM Horizontal, harmonic mixing coefficient (m ² /s) for tracer 01: temp
5.0000E+01	nl_tnu2(02)	NLM Horizontal, harmonic mixing coefficient (m ² /s) for tracer 02: salt
5.0000E+01	ad_tnu2(02)	ADM Horizontal, harmonic mixing coefficient (m ² /s) for tracer 02: salt
5.0000E+01	tl_tnu2(02)	TLM Horizontal, harmonic mixing coefficient (m ² /s) for tracer 02: salt
1.0000E+01	nl_visc2	NLM Horizontal, harmonic mixing coefficient (m ² /s) for momentum.
1.0000E+01	ad_visc2	ADM Horizontal, harmonic mixing coefficient

		(m2/s) for momentum.
1.0000E+01	tl_visc2	TLM Horizontal, harmonic mixing coefficient (m2/s) for momentum.
	T LuvSponge	Turning ON sponge on horizontal momentum.
	T LtracerSponge(01)	Turning ON sponge on tracer 01: temp
	T LtracerSponge(02)	Turning ON sponge on tracer 02: salt
1.0000E-06	Akt_bak(01)	Background vertical mixing coefficient (m2/s) for tracer 01: temp
1.0000E-06	Akt_bak(02)	Background vertical mixing coefficient (m2/s) for tracer 02: salt
1.0000E-05	Akv_bak	Background vertical mixing coefficient (m2/s) for momentum.
5.0000E-06	Akk_bak	Background vertical mixing coefficient (m2/s) for turbulent energy.
5.0000E-06	Akp_bak	Background vertical mixing coefficient (m2/s) for turbulent generic statistical field.
	2.000 gls_p	GLS stability exponent.
	1.000 gls_m	GLS turbulent kinetic energy exponent.
	-0.670 gls_n	GLS turbulent length scale exponent.
7.6000E-06	gls_Kmin	GLS minimum value of turbulent kinetic energy.
1.0000E-12	gls_Pmin	GLS minimum value of dissipation.
5.2700E-01	gls_cmu0	GLS stability coefficient.
1.0000E+00	gls_c1	GLS shear production coefficient.
1.2200E+00	gls_c2	GLS dissipation coefficient.
5.0000E-02	gls_c3m	GLS stable buoyancy production coefficient.
1.0000E+00	gls_c3p	GLS unstable buoyancy production coefficient.
8.0000E-01	gls_sigk	GLS constant Schmidt number for TKE.
1.0700E+00	gls_sigp	GLS constant Schmidt number for PSI.
	1400.000 charnok_alpha	Charnok factor for Zos calculation.
	0.500 zos_hsig_alpha	Factor for Zos calculation using Hsig(Awave).
	0.250 sz_alpha	Factor for Wave dissipation surface tke flux .
	100.000 crgban_cw	Factor for Craig/Banner surface tke flux.
1.0000E+00	ad_Akt_fac(01)	ADM basic state vertical mixing scale factor for tracer 01: temp
1.0000E+00	tl_Akt_fac(01)	TLM basic state vertical mixing scale factor for tracer 01: temp
1.0000E+00	ad_Akt_fac(02)	ADM basic state vertical mixing scale factor for tracer 02: salt
1.0000E+00	tl_Akt_fac(02)	TLM basic state vertical mixing scale factor for tracer 02: salt
1.0000E+00	ad_Akv_fac	ADM basic state vertical mixing scale factor for momentum.
1.0000E+00	tl_Akv_fac	TLM basic state vertical mixing scale factor for momentum.
3.0000E-04	rdrg	Linear bottom drag coefficient (m/s).
3.0000E-03	rdrg2	Quadratic bottom drag coefficient.
2.0000E-02	Zob	Bottom roughness (m).
2.0000E-02	Zos	Surface roughness (m).
2.0000E+00	blk_ZQ	Height (m) of surface air humidity measurement.
2.0000E+00	blk_ZT	Height (m) of surface air temperature measurement.
1.0000E+01	blk_ZW	Height (m) of surface winds measurement.
	5 lmd_Jwt	Jerlov water type.
	2 Vtransform	S-coordinate transformation equation.
	4 Vstretching	S-coordinate stretching function.
6.0000E+00	theta_s	S-coordinate surface control parameter.
3.0000E-01	theta_b	S-coordinate bottom control parameter.
	100.000 Tcline	S-coordinate surface/bottom layer width (m) used in vertical coordinate stretching.
	1025.000 rho0	Mean density (kg/m3) for Boussinesq approximation.
1.0000E-05	bvf_bak	Background Brunt-Vaisala frequency squared (1/s2).
	17804.000 dstart	Time-stamp assigned to model initialization (days).
	0.000 tide_start	Reference time origin for tidal forcing (days).
19700101.00	time_ref	Reference time for units attribute (yyyymmdd.dd)
5.0000E+00	Tnudg(01)	Nudging/relaxation time scale (days) for tracer 01: temp
5.0000E+00	Tnudg(02)	Nudging/relaxation time scale (days) for tracer 02: salt
0.0000E+00	Znudg	Nudging/relaxation time scale (days)

		for free-surface.
0.0000E+00	M2nudg	Nudging/relaxation time scale (days) for 2D momentum.
5.0000E+00	M3nudg	Nudging/relaxation time scale (days) for 3D momentum.
3.0000E+01	obcfac	Factor between passive and active open boundary conditions.
	F VolCons(1)	NLM western edge boundary volume conservation.
	F VolCons(2)	NLM southern edge boundary volume conservation.
	F VolCons(3)	NLM eastern edge boundary volume conservation.
	F VolCons(4)	NLM northern edge boundary volume conservation.
	F ad_VolCons(1)	ADM western edge boundary volume conservation.
	F ad_VolCons(2)	ADM southern edge boundary volume conservation.
	F ad_VolCons(3)	ADM eastern edge boundary volume conservation.
	F ad_VolCons(4)	ADM northern edge boundary volume conservation.
	F tl_VolCons(1)	TLM western edge boundary volume conservation.
	F tl_VolCons(2)	TLM southern edge boundary volume conservation.
	F tl_VolCons(3)	TLM eastern edge boundary volume conservation.
	F tl_VolCons(4)	TLM northern edge boundary volume conservation.
14.000	TO	Background potential temperature (C) constant.
35.000	S0	Background salinity (PSU) constant.
1.7000E-04	Tcoef	Thermal expansion coefficient (1/Celsius).
0.0000E+00	Scoef	Saline contraction coefficient (1/PSU).
1.000	gamma2	Slipperiness variable: free-slip (1.0) or no-slip (-1.0).
	T LuvSrc	Turning ON momentum point Sources/Sinks.
	F LwSrc	Turning OFF volume influx point Sources/Sinks.
	F LtracerSrc(01)	Turning OFF point Sources/Sinks on tracer 01: temp
	T LtracerSrc(02)	Turning ON point Sources/Sinks on tracer 02: salt
	F LsshCLM	Turning OFF processing of SSH climatology.
	F Lm2CLM	Turning OFF processing of 2D momentum climatology.
	F Lm3CLM	Turning OFF processing of 3D momentum climatology.
	F LtracerCLM(01)	Turning OFF processing of climatology tracer 01: temp
	F LtracerCLM(02)	Turning OFF processing of climatology tracer 02: salt
	F LnudgeM2CLM	Turning OFF nudging of 2D momentum climatology.
	F LnudgeM3CLM	Turning OFF nudging of 3D momentum climatology.
	F LnudgeTCLM(01)	Turning OFF nudging of climatology tracer 01: temp
	F LnudgeTCLM(02)	Turning OFF nudging of climatology tracer 02: salt